SPIE. SCANNING MICROSCOPIES

CONNECTING MINDS.
ADVANCING LIGHT.

2014

SCANNING MICROSCOPIES.

TECHNOLOGY
SUMMARIES

WWW.SPIE.ORG/SG

Monterey Conference Center
Monterey, California, USA

Exhibition: 16–17 September 2014

Conference: 16-18 September 2014

CO-LOCATED WITH
SPIE PHOTOMASK TECHNOLOGY 2014.

SPIE.

2014 SCANNING MICROSCOPIES.

SYMPOSIUM CHAIRS

Michael T. Postek
National Institute of Standards and Technology

Dale E. Newbury
National Institute of Standards and Technology

S. Frank Platek
U.S. Food and Drug Administration

Tim K. Maugel
Univ. of Maryland, College Park

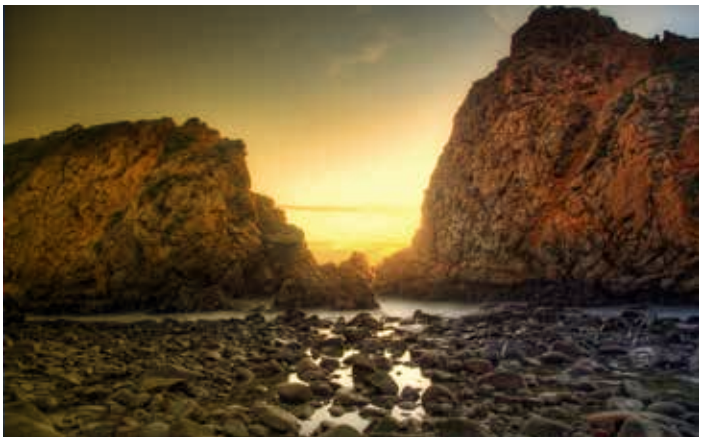

Contents

SPIE.

9236-1, Session 1

3D Monte Carlo modeling of the SEM: Are there applications to photomask metrology? *(Invited Paper)*

John S. Villarrubia, András E. Vladár, Michael T. Postek, National Institute of Standards and Technology (United States)

To determine feature width from a scanning electron microscope (SEM) image, the usual procedure relies upon image processing techniques. The feature edge, which is characterized by a bright bloom, is assigned a position typically based upon where the intensity crosses a threshold or where the gradient of the intensity is greatest. At the nanometer scale, there are issues of accuracy and reproducibility with this approach: (1) Owing to the finite escape depth of electrons in the sample, the bloom is some nanometers wide. Different edge assignment methods therefore make nanometer differences in the measured widths. At most one of these can be correct. (2) In addition to the feature width, the shape and position of the bloom depends upon the composition and shape of the edge, the proximity of neighboring objects on the sample, and other “secondary” sample characteristics. Some of the apparent width variation site to site or among batches is actually variation of these secondary characteristics.

Model-based metrology is an alternative approach. The width and other unknown parameters are assigned by fitting an equation of the form I(x,y) = M(x,y;p), where I(x,y) is the measured SEM image and M(x,y;p) is a physics-based model that predicts the image given a vector of parameters, p, that characterize the instrument and the sample. These include the feature width but also other parameters (e.g., sidewall angle, corner rounding, proximity of neighbors,…) that affect the intensity. By accounting for secondary characteristics separately, this method reduces their influence on the measurement of the desired primary characteristic. It also measures these secondary characteristics, thereby enabling applications in which one or more of these become the primary measurands.

When we introduced this method for SEM metrology about a decade ago [review: Villarrubia et al, Surf. Interface Anal. 37, 951-958 (2005)] M(x,y;p) was based on MONSEL (MONte Carlo simulator for Secondary ELectrons). A newer code, JMONSEL (Java MONSEL), allows considerably more flexibility in the definition of arbitrary 3D sample shapes and updates much of the physics. The code simulates electron scattering (with nuclei, other electrons including secondary electron generation, or phonons), refraction at material boundaries, transport (including in electric fields caused by charging), trapping, and detection. Because simulation is computation-intensive, only a discrete set of parameter values that form a regular grid in parameter space in the neighborhood of the expected parameter values are simulated. The resulting “library” is interpolated. The interpolation function becomes a fast, continuous, and (provided the grid is fine enough) accurate surrogate for the Monte Carlo model. The fit can be performed by standard nonlinear least squares algorithms, e.g., Levenberg-Marquardt. We have recently used this method to determine the size and shape of 10 nm asymmetric silicon nitride features on a layered substrate. The measurement results compared favorably with results by TEM and small angle x-ray scattering on the same or sister targets.

In this paper we review the current state of Model-based SEM measurement as used for wafer metrology, and then explore its applicability to mask metrology. Are there unique issues? What, if any, new modeling capabilities would be required to extend this technique to mask metrology?

9236-2, Session 2

3D isotropic reconstruction of biological samples through cycles of physical and virtual sectioning in electron microscopy

Ben Lich, Faysal Boughorbel, Pavel Potocek, Liesbeth Hekking, Ron van den Boogaard, Emine Korkmaz, Pavel Cernohorsky, FEI Electron Optics, B.V. (Netherlands); Milos Hovorka, FEI Co. (Czech Republic); Matthias Langhorst, FEI Co. (Germany)

In recent years there has been a considerable advancement in SEM-based methods for 3D reconstruction of large tissue volumes. Serial Block-Face SEM (SBF-SEM) involves combination of imaging and in-situ sectioning of plastic embedded tissue blocks within the SEM vacuum chamber1, allowing for automated imaging and subsequent reconstruction of volumes of tissue. The use of low electron energies for imaging limits sample charging which can be further mitigated with imaging in low vacuum mode and by further increasing the conductivity of the sample through sufficient amount of heavy metal staining and in-situ metal coating of the block face.

Here we introduce a novel solution for high spatial resolution and throughput SEM volume imaging overcoming the resolution limits set by mechanical slicing by combining it with virtual sectioning. Virtual slicing is realized by Multi-Energy Deconvolution SEM (MED-SEM), a non-destructive technique that allows high resolution reconstruction of the top layers of the sample.2 After cutting a thin layer of the blockface using a diamond knife, freshly exposed tissue is imaged several times using various accelerating voltages. These images are subsequently used for deconvolving the information into several virtual subsurface layers. This cycle of physical and virtual sectioning offers isotropic datasets with excellent z-resolution and can be fully integrated and automated.

9236-3, Session 2

A novel approach for scanning electron microscopic observation in atmospheric pressure

Yusuke Ominami, Shinsuke Kawanishi, Hitachi High-Technologies Corp. (Japan); Tatsuo Ushiki, Niigata Univ. (Japan); Sukehiro Ito, Hitachi High-Technologies Corp. (Japan)

The scanning electron microscope (SEM) has been used as a powerful tool for providing surface information of micro and nanostructures. Because the conventional SEM being operated under a vacuum condition, wet samples require drying before SEM observation. To overcome this inconvenience, efforts has been devoted to designing environmental and low vacuum SEMs, which enable imaging samples in gaseous and vapor conditions with the pressure range from 100 Pa to 103 Pa. In recent years, SEM methods for observing wet samples under atmospheric pressure have been reported by some investigators. With these methods, the sample space is separated by a thin transparent membrane from vacuum environment where electron beam is propagated. Also, samples attaching to the membrane are observed by SEM.

In the present study, we developed a table-top atmospheric SEM (ASEM) for observing samples which are kept in ambient air conditions but are separated from the membrane. Our ASEM has an inner chamber inside a regular specimen chamber. This inner chamber is equipped with an attachable thin membrane on its roof. When a sample should be exchanged, the specimen stage is extracted from the inner chamber. In this configuration, the environment around the sample can be kept in ambient air conditions and changed by evaporation with an additional vacuum pump. Moreover, the higher vacuum observation can be also performed after removing the membrane from the inner chamber. This means that our ASEM enables observation of samples under not only atmospheric but also various-ranged vacuum pressures.

Using our ASEM, we observed wet regenerated cellulose fibers at atmospheric pressure. After obtaining an image of wet fibers, the specimen chamber was evacuated using the additional vacuum pump and the same fibers were observed in different pressure conditions. Measurement from the SEM images shows that the fibers shrunk approximately 25 % in diameter after evaporation, indicating that the fibers swell with water. We also succeeded in observing wet biological samples including mildew fungus, blood cells and renal glomerulus at atmospheric pressure using light microscope and our ASEM. Since no additional preparation of samples are required between light microscope and our ASEM observation, the technique allows to be widely used for evaluation of various materials. We show some examples of these SEM images and discuss the future of this technique for applying to studies on three-dimensional surface structure of samples by SEM in ambient atmospheric conditions.

9236-4, Session 2

Does your SEM really tell the truth? How would you know? part 3: vibration and drift

Michael T. Postek, Andras E. Vladár, National Institute of Standards and Technology (United States); Petr Cizmar, Physikalisch-Technische Bundesanstalt (Germany)

This is the third of a series of presentations discussing various contributions to the measurement uncertainty in scanned particle beam instruments and some of the solutions researched at NIST. Scanned particle beam instruments especially the scanning electron microscope (SEM) have gone through tremendous evolution to become critical tools for many and diverse scientific and industrial applications. These improvements have significantly improved the overall SEM performance and have made the instrument far easier to operate. But, ease of operation has also fostered operator complacency. In addition, the user friendliness has reduced the “apparent” need for more thorough operator training for using of these instruments. Therefore, this overall attitude has fostered the concept that the SEM is just another expensive digital camera or another peripheral device for a computer and that all of the issues related to obtaining quality data have been solved. Hence, a person using these instruments may be lulled into thinking that all of the potential pitfalls have been fully eliminated and they believe everything they see on the micrograph is always correct. But, as described in this and the earlier presentations this may not be the case. The first paper in this series, discussed some of the issues related to signal generation in the SEM, including instrument calibration, electron beam interactions and the need for physics-based modelling to accurately understand the actual image formation mechanisms. All these were summed together in a discussion of how these issues effect measurements made with the instrument. The second paper, discussed another major issue confronting the microscopist: specimen contamination and methods of contamination elimination. This third presentation discusses vibration and drift and some possible solutions. Over the years, workers at NIST have done a great deal of research into these issues in order to improve the fundamental metrology and some of this work is reviewed and discussed here.

9236-5, Session 2

Scanning electron microscopy menagerie *(Invited Paper)*

Vladimir Vishnyakov, Manchester Metropolitan Univ. (United Kingdom)

Many materials have complicated composition and atomic structure and their examination is extremely challenging. Different signals can be processed within a Scanning Electron Microscope (SEM) and comprehensiveness of analysis can be further enhances by inclusion of structure sensitive methods such as Electron Backscattering Diffraction (EBSD) and micro-Raman. Addition of Cathodoluminescence (CL), Variable Pressure and Cold stage does allow for all-inclusive analysis of unperturbed by preparation samples. Such a system on a single SEM has been created few years ago and allowed to study wide ranging set of samples stretching from environmental pollution particles and microorganisms to drugs and advanced ceramics.

9236-7, Session 3

Investigations on CMOS photodiodes using scanning electron microscopy with electron-beam induced current measurements (SEM-EBIC)

Andrea Kraxner, ams AG (Austria) and Technische Univ. Graz (Austria); Frederic Roger, Bernhard Loeffler, ams AG (Austria); Peter Hadley, Technische Univ. Graz (Austria); Rainer Minixhofer, ams AG (Austria); Martin Faccinelli, Technische Univ. Graz (Austria)

Electron beam induced current (EBIC) is a scanning electron microscopy measurement (SEM) technique where micro probes are used together with a scanning electron microscope. An electron beam is scanned over a semiconductor sample. Where the electron beam interacts with the semiconductor, secondary electron cascades and electron-hole pairs are generated. With the presence of a junction like a p-n junction or Schottky junction the electron-hole pairs get separated by the associated electric field and an excess current is flowing – the so-called electron beam induced current. This current is collected by the probes, amplified and analyzed either as a function of the beam position or as a function of time. [1].

EBIC is a powerful tool used in several different areas. Some common applications are the identification and analysis of defects and the failure analysis for semiconductor devices like discussed in [2] and [3]. Another important field is to investigate recombination and transport properties of semiconductors and semiconductor devices, which has been published for solar cells ([4] and [5]).

In this work EBIC is used to evaluate CMOS photodiodes. Standard CMOS processes provide a wide range of different possible photodiode designs, by simple combination of semiconductor wells and diffusions. This gives the possibility to choose from a variety of structures, selecting the best solution for a specified application. Within this context EBIC is a very suitable tool to get complementary information next to electric and optical characteristics.

Experimental designs of vertical pn-diode structures are specifically designed to closely resemble junction configurations where an analytical solution exists (e.g. step-junction and grade-junction). Different substrate configurations (standard silicon p-- substrate and p—substrate with highly doped ++ background) are processed in an epitaxial reactor for the purpose of deposit the designed junction profile. Special care has been taken to minimize the thermal budget to get closer to the analytical junction solutions.

These structures are then investigated with respect to the influence of junction position, doping concentration and biasing on the electric field and the current flow in the device. The EBIC current is measured and analyzed. It is demonstrated that the position and the width of the space charge region, the electric field distribution and the minority carrier diffusion length can be extracted from the EBIC results and match fairly well to the analytical solutions.

In addition to the measurements, three dimensional technology computer aided design (TCAD) simulations of the EBIC measurement process are done for the first time to analyze the real junction configuration more in detail. Furthermore the TCAD method provides direct access to the spatial distribution of physical quantities (like mobility, lifetime etc.) which are very difficult to obtain experimentally. The simulations are in good agreement with the experimental EBIC measurements. A comparison of the extracted junction parameters (e.g. the diffusion length, space charge region structure) is done between analytical results, EBIC measurements and TCAD simulations.

It is demonstrated that the combination of EBIC measurements and

TCAD simulations results in much better insight into the internal function of diodes enabling more efficient optimization and design of diode structures such as photodiodes.

[1] “Scanning Electron Microscopy – Physics of Image Formation and Analysis”, L. Reimer, 2nd Edition, 1998, Springer Verlag

[2] “The origin of EBIC defect contrast in silicon”, M. Kittler und W. Seifert, physica status solidi, 1993

[3] “EBIC investigations of dislocations and their interactions with impurities in silicon”, T.S. Fell et al, physica status solidi, 1993

[4] “Determination of Minority-Carrier Lifetime and Surface Recombination Velocity with High Spacial Resolution”, M. Watanabe et al, IEEE Transactions on electron devices, Vol. ed-24, 1977

[5] “Theory of beam induced current characterization of grain boundaries in polycrystalline solar cells”, C. Donotato, Journal of Applied Physics 54, 1983!!

9236-8, Session 3

A novel transmission electron-imaging technique for observation of samples on plate using scanning electron microscope

Yusuke Ominami, Hitachi High-Tech Science Corp. (Japan); Masato Nakajima, Tatsuo Ushiki, Niigata Univ. (Japan); Sukehiro Ito, Hitachi High-Tech Science Corp. (Japan)

The ultrastructure of biological tissues and cells has been studied mainly by transmission electron microscopy (TEM) and scanning transmission electron microscopy (STEM). For this purpose, samples usually need to be embedded in plastic resin and cut into ultrathin sections for mounting them onto mesh grids. Meanwhile, correlative light and electron microscopy (CLEM) for observing same samples using light and electron microscope has been also recently reported by some investigators. By light microscopy, samples are normally placed on a transparent plate (i.e., a glass slide or a dish), which makes it difficult to investigate the internal structure using TEM and STEM. Thus, by CLEM, the observed sample has to be further sliced into ultrathin sections and placed on mesh grids after observation with a light microscope. To overcome this technical complexity, we propose, in this study, a novel and simple technique for transmission electron imaging by scanning electron microscopy (SEM) for observing samples on plate. In this technique, samples are placed on a transparent and flat plate in advance which is made of a scintillator material that emits photons by electron irradiations. Electrons are backscattered by internal structures of the samples with higher density or penetrated into structures with lower density, thus generating the varying number of photons from the plate. As a result, the contrast of obtained image is produced by transmitted electrons (TEs).

In order to evaluate the utility of the proposed technique, muntjac cells (MM2T) were cultivated on the scintillator plates in microplate wells. After cultivation, the samples were fixed in 1% glutaraldehyde and stained with 1% OsO4, dehydrated in a ETOH series and critical point-dried. The SEM used in this study was a Hitachi SU3500 tungsten emission SEM with a photo detector. This technique enables the wide-field observation of whole cells at lower magnification because all cells are directly placed not on mesh grid but on a plate for detecting TEs. This TE image with internal cell information can be clearly compared with the image obtained by secondary electrons (SEs), which has information on the cell surface structure. High magnification images clearly show structures inside cells. Stereo-pair images can be obtained by tilting an incident electron beam at ±5o. In conclusion, the proposed technique is very useful for obtaining TE images of whole cells with a conventional SEM without use of any destructive sample-thinning process. In this presentation, the transmission imaging mechanism and obtained images are introduced.

9236-53, Session 3

Three-dimensional surface reconstruction using scanning electron microscopy and the design of a nanostructured electron trap

Renke Scheuer, Eduard Reithmeier, Leibniz Univ. Hannover (Germany)

This paper gives an overview of the possible methods for a three-dimensional surface acquisition in the micrometer scale. It is pointed out that Scanning Electron Microscopy is a capable method for measurement tasks of this kind; therefore, it presents possible ways for implementing this technique in a three-dimensional surface reconstruction. The improved photometric method promises the best performance; its further implementation is developed and explained. Therefore, some modifications of the employed Scanning Electron Microscope (SEM) are described, for instance, the integration of two supplemental detectors, a modified collector grid and a gun shielding. All modifications were evaluated using FEM-Simulations before their implementation. A signal mixing is introduced in order to still be able to use the improved photometric method with four detectors in spite of the fact that it was designed for a two-detector system.

For verification purposes, a sphere normal is measured by means of the modified system. It can be seen that the maximal detectable slope angle could be increased compared to the old photometric method. In addition, we introduce an electron trap made from nanostructured titanium. The structure is tested regarding its ability to catch electrons of different energies and compared to non-structured titanium. The trap can later be implemented on the bottom of the electron gun to catch unwanted backscattered electron (BSE) emission which could otherwise affect the three-dimensional reconstruction.

9236-10, Session 4

Shear force microscopy using piezoresistive cantilevers in surface metrology

Teodor P. Gotszalk, Daniel Kopiec, Wroclaw Univ. of Technology (Poland); Andrzej Sierakowski, Pawel Janus, Piotr B. Grabiec, Institute of Electron Technology (Poland); Ivo W. Rangelow, Technische Univ. Ilmenau (Germany)

Atomic force microscopy (AFM) belongs to the technologies, which enable high resolution investigations and modifications of surface properties. Despite its high sensitivity, which enables imaging of atomic structures, the standard AFM applications are restricted to small area specimens. In addition, the relatively long time of the imaging or modification process makes the usage of the AFM-based technology in industrial applications limited. The routine AFM investigations are usually performed on flat samples, which Is the another constraint in measurements of technological samples, on which details with big height differences should often be imaged. From that point of view standard AFM solution based on optical beam deflection (OBD) detector and cantilevers with microtips integrated at the end of the spring beam are often not acceptable in the measurements of technological samples. In this paper we describe technology applying a piezoresistive cantilever with planar probes in Shear Force Microscopy (ShFM), which is one of the AFM technologies. In the ShFM investiagtions the force interactions are focused at the tip planarly protruding of the spring beam. In contrast to the standard AFM investigations, the microtip vibrates laterally to the investigated sample. In this way, the microtip can penetrate deep structures and samples containing features of bigger height can be imaged with the resolution ensured by the standard AFM technology. Additionally, it should be noted that the fabrication process of the ShFM cantilevers is simplified in contrast to the fabrication process of the standard AFM cantilevers, which integrates the vertical 3 dimensional (3D) microtip.

In our solution we applied the piezoresitive detection scheme to detect the cantilever vibration. The piezoresistive microcantilevers are widely

applied in measurements of low forces, masses and viscosity due to their high sensitivity [1], [2]. Because the deflection signal is sensed electronically, the design and fabrication of elaborate AFM systems is simplified. In addition, integration of thermal actuator with the piezoresistive cantilevers opens the possibility to control the cantilever tip deflection and increase surface metrology and lithography throughput [3], [4]. It should be underlined, that the piezoresistive cantilevers belong to the only few micro electro mechanical systems (MEMS), which enable metrological (in other words quantitave) force and deflection investigations [5], [6]. The unique features presented here make thermally actuated piezoresistive cantilever applied in the ShFM the best technology for precise metrology of technological samples. However, a reliable application of the solution described requires profound analysis of the system properties. In this article it will be presented, how to calibrate the detection and actuation sensitivity of the piezoresistive beam. In the described procedures advanced interferometrical methods are used to determine the deflection sensitivity. The determination of the cantilever spring constant is based on the analysis of the thermomechanical fluctuation of the micromechanical beam, which limits the minimal detectable force acting at the microtip. The spring constant obtained on the basis of the noise analysis was compared with spring constant values calculated on the basis of spring beam resonance frequency and its geometry. The architecture of the AFM based system for the surface metrological investigations, which utilizes the thermally actuated piezoresistive probes will be introduced [7], [8]. The results of the surface measurements using the ShFM piezoresistive cantilevers will be also presented.

[1] T. Gotszalk, P.Grabiec, I. Rangelow, Piezoresistive sensors for scanning probe microscopy, Ultramicroscopy, 82, 39, 2000.

[2] M. Woszczyna, P. Zawierucha, P. Pa?etko, M. Zielony, T. Gotszalk, Y. Sarov, T. Ivanov, A. Frank, J. Zöllner, I. W. Rangelow, Micromachined scanning proximal probes with integrated piezoresistive readout and bimetal actuator for high eigenmode operation, J. Vac. Sci. Technol., B 28„6, Nov/Dec 2010, 2010.

[3] I.W. Rangelow, Tzv. Ivanov, K. Ivanova, B.E. Volland, Y. Sarov, A. Persaud, H.P. Reithmaier, T. Gotszalk, P. Zawierucha, M. Zielony, D. Dontzov, B. Schmidt, M. Zier, N. Nikolov, I. Kostic, W. Engl, T. Sulzbach, J. Mielczarski, S. Kolb, Du P. Latimier, R. Pedreau, V. Djakov, S.E. Huq, K. Edinger, O. Fortagne, A. Almansa and H.-O. Blom, Piezoresistive and Self-Actuated 128-Cantilever Arrays for Nanotechnology Applications, Microelectronic Engineering Volume 84, Issues 5-8, (2007) Pages 1260-1264.

[4] A. Frank, J.-P. Zöllner, Ch. Bitterlich, U. Wenzel, B.E. Volland, S. Klett ,I.W. Rangelow, P. Zawierucha, M. Zielony , T. Gotszalk, D. Dontzov ,W. Schott, N. Nikolov, M. Zier, B. Schmidt, W. Engl, T. Sulzbach and I. Kostic, Scanning proximal probes for parallel imaging and lithography, K. Ivanova, Y. Sarov, Tzv. Ivanov, , J. Vac. Sci. Technol. B 26(6), Nov/Dec 2008, pp. 2367-2373.

[5] M. Woszczyna, P. Zawierucha, M. ?wi?tkowski, T. Gotszalk, P. Grabiec, N. Nikolov, J. Mielczarski, E. Mielczarska, N. Glezos, Tzv. Ivanow, K. Ivanowa, Y. Sarov, I.W. Rangelow, Quantitative force and mass measurements using the cantilever with integrated actuator and deflection detector, Microelectronic Engineering, 86, 1043-1045, 2009.

[6] M. Woszczyna, T. Gotszalk, P. Zawierucha, M. Zielony, Tzv. Ivanow, K. Ivanowa, Y. Sarov, N. Nikolov, J. Mielczarski, E. Mielczarska, I.W. Rangelow Thermally driven piezoresistive cantilevers for shear-force microscopy, Microelectronic Engineering, 86, 4–6,1212-1215, 2009.

[7] Zahid Durrani, Marcus Kaestner, Manuel Hofer, Tzvetan Ivanov, and Ivo Rangelow, Scanning probe lithography for electronics at the 5nm scale, SPIE NEWSROOM, 10.1117/2.1201302.004653.

[8] N. Vorbringer-Doroshovets, F. Balzer, R. Fuessl, and Eberhard Manske, M. Kaestner, A. Schuh, J. Zoellner, M. Hofer, E. Guliyev, A. Ahmad, Tz. Ivanov, and I.W. Rangelow , 0.1-nanometer resolution positioning stage for sub-10 nm scanning probe lithography, , Proc. of SPIE Vol. 8680 868018-1.

9236-11, Session 4

High-throughput data acquisition with a multi-beam SEM

Anna Lena Keller, Dirk Zeidler, Thomas Kemen, Carl Zeiss Microscopy GmbH (Germany)

The maximum usable data acquisition rate of scanning electron microscopes is ultimately given by the electron dose per pixel required to generate a desired signal to noise ratio. This dose is determined by pixel dwelling time and beam current. The signal to noise ratio also depends on sample properties and detection efficiency. Therefore, the speed of conventional SEMs is limited, as (i) increasing the beam current will ultimately cause increasing Coulomb interactions, thereby blurring the electron beam and reducing the resolution at the sample, (ii) the dwelling time per pixel is ultimately limited by the band width of electron detectors, and (iii) the detection efficiency cannot exceed 100%.

We use multiple parallel electron beams in a single column to bypass the detector bandwidth limit and alleviate Coulomb interaction limitations. A regular array of electron beams is imaged onto the sample and forms a pattern of primary electron spots. The secondary electrons that emanate from each primary electron spot are then projected onto a multi-detector. A magnetic beam splitter separates primary and secondary electron beams. The bundle of electron beams is scanned over the sample, and the secondary electron yield is recorded for each scan position, just as in any conventional SEM. One single scanning pass thus produces multiple images in parallel, yielding a complete image of the field of view underneath the primary beam array.

Hence, the total possible detector bandwidth is the single detector bandwidth multiplied by the number of beams. Due to the decreased current per beam, the Coulomb interaction is much lower than in a single-beam configuration of comparable overall current.

The dramatic increase of imaging speed opens the door for electron microscopy to applications where both high resolution and large scan area are of key importance. This will be, for example, the case for applications where high resolution has been classically required, but large area scanning has been impossible up to date, as well as applications that require large area acquisition and up to now therefore had to be accomplished using light optical techniques.

9236-12, Session 4

On the limits of miniature electron column technology

Lawrence P. Muray, James P. Spallas, Agilent Technologies, Inc. (United States)

Miniature columns or microcolumns are a relatively new class of electron beam columns fabricated entirely from silicon using advanced micromachining processes. The main characteristics of these columns are thermal field emission (TFE) sources, low voltage operation (typically <3keV), simple design (two lenses, no crossover), microfabricated lenses, and all electrostatic components. Current production versions of miniature columns achieve <10nm resolution at 1keV, and have demonstrated <6nm resolution at higher beam energies1. While this performance is suitable for many applications, previous studies show the electron optics of miniature electrostatic lenses are capable of better performance under ideal conditions2. Achieving these ideal conditions in practice is challenging because the miniature optics must be combined with other subsystems which impose additional constraints. An understanding of these major contributors to column performance, whether optical or mechanical, is essential, and can provide a roadmap for further improvements in the existing technology.

The major limitations of miniature column performance are due to competing requirements to minimize optical aberrations, relax physical or geometric constraints (e.g. working distance, electrode-electrode distance), and maintain manufacturable mechanical tolerances (e.g.,

alignment, diameter, and placement) of the column components. Achieving the best balance of these three categories produces the best performance, and improvement in any one of these categories is an opportunity to re-optimize the system. An example of the impact of misalignments relative to the optical axis on beam blur for a typical miniature column design is shown in Fig. 1. Each line represents the effect of a single silicon lens element misalignment. Depending on the particular optical element, a single element misalignment of 10 um can be either inconsequential or lead to a doubling of the beam full width half maximum (FWHM). Further miniaturization of the lens elements can exacerbate the blur and adding multiple elements in quadrature can result in unusable columns. To develop a good understanding of expected alignment errors, estimate column yield and, most importantly, guide the column design, a Monte Carlo method was developed to simulate typical blurring profiles based on assembly techniques.

This method, along with specific results will be discussed in the presentation. Other constraints will be discussed along with ideas to improve the current state-of-the-art.

1J.P. Spallas, C. S. Silver, L.P. Muray, T. Wells, and M. El Gomati, “A Manufacturable Miniature Electron Beam Column,” Microelectron. Eng. 83, 984-989, (2006).

2 T.H.P. Chang, D.P. Kern, and L.P. Muray, “Microminiaturization of Electron Optical Systems”, J. Vac. Sci. Technol. B 8(6), 1698-1705 (1990).

9236-13, Session 4

Hybrid metrology method for improving LWR/LER measurement in CD-SEM images

Nivea G. Figueiro, CNRS-LTM (France) and Univ. Grenoble Alpes-LTM (France) and CEA-LETI (France); Marc Fouchier, Erwine Pargon, CNRS-LTM (France); Maxime Besacier, Univ. Grenoble Alpes-LTM (France); Jérome Hazart, Sandra Bos, CEA-LETI (France)

The semiconductor industry continues to evolve in its never ending reduction of feature sizes. As devices shrink, the control of critical dimensions (CDs) and feature profiles has become a key for ensuring optimal device performance and high production yield. Moreover, as the CD becomes smaller, the impact of line roughness on device performance variability gains importance [1]. An accurate line roughness measurement technique is thus mandatory for semiconductor process optimization, for the development of next-generation lithography and for the prediction of device performance.

The industry has developed different techniques for measuring line roughness, being the most widely used one critical dimension-scanning electron microscopy (CD-SEM). CD-SEM is a fast and nondestructive method designed for inline metrology. However, the high noise in the acquired images induces a bias from true roughness [2,3]. Recently, it was developed a method based on atomic force microscopy (AFM) that provides more accurate line roughness measurements thanks to its low noise images. In this method, the sample is tilted at about 45º and the feature is scanned along its length with a small radius tip which results in high resolution images. Moreover, this method permits the measurement of the roughness all along the feature height [4].

In this paper it is shown that filtering CD-SEM images before the edge detection provides more accurate edge roughness measurements. However the selection of the filtering algorithm and its parameters is crucial for obtaining an accurate roughness measurement. A weak filter will fail to significantly reduce the image noise, while an aggressive filter will remove relevant roughness information. Figure 1 shows the estimation of a feature contour calculated over a) a non-filtered image, b) a properly filtered image and c) an overly filtered image. These exemple clearly show that the final roughness measurement will depend on the applied filter in the pre-processing step.

Determining the most adequate filtering strategy for CD-SEM images is a challenging task, especially when a large volume of data is handled and only a fully automated approach is conceivable. In this context, a method for calibrating the image treatment algorithms was developed, in order to improve CD-SEM measurements. It relies on the use of the results obtained by tilted AFM as a reference, in a hybrid metrology approach.

The experimental data were acquired using a Hitachi CG4000 CD-SEM and a Bruker Dimension Icon AFM with a modified sample holder. Several photoresist and silicon patterns were measured by both methods. CD-SEM images with various initial noise levels were obtained by varying the number of acquisition frames. The images were then treated with Median and Gaussian filters, varying their parameters. The images were then processed by a dedicated algorithm for edge detection and roughness estimation, which was also developed in this project and is described in the article. The obtained edge roughness values were then compared with the values measured by AFM to determine the best filter parameters.

9236-44, Session PS1

A tale of three trials: from science to junk science

Bryan R. Burnett, Meixa Tech (United States)

The defendant, a residential building contractor, was tried and convicted for the murders of his brother and sister-in-law which occurred in a coastal California city in 2009. He had three trials. The first ended in mistrial due to a witness’ inappropriate statement while on the stand. The second ended in a mistrial due to a hung jury and the third, he was convicted. Examination of the gunshot residue (GSR) evidence presented in the first and the third trials starkly defined an extraordinary difference between the two.

The evidence:

1) Hand sampling for GSR occurred 8.5 hours after the shooting and were taken at a police station. No protection (i.e., hand bagging) from police environment contamination was provide and no controls were taken at the police station.

2) Gloves and a fanny pack believed to have been worn by the defendant during the shootings.

3) The interior of a pickup truck believed to have been driven by the defendant immediately after the shooting.

The first trial: The expert presented by the prosecution was new to GSR analysis and testimony. The data she presented were reliable and the entire samplers were analyzed. Her data was, as will be described in this presentation, exculpatory when it was analyzed by the author.

The third trial: The prosecution’s GSR expert of the first and second trials was unavailable. Consequently, a new GSR expert reanalyzed the GSR evidence. He also analyzed the particle generation from construction power hammers which were in the possession of the defendant. The data he presented will be shown to be unreliable, fragmented, incomplete and ultimately misleading. The junk science taken at face value was inculpatory. There was no defense GSR expert rebuttal despite the defense attorney knowing the content of the author’s GSR analysis from the first trial’s GSR expert as well as his report concerning the prosecution’s second GSR expert.

The author shows, using the data from the first expert, that the characteristic GSR population from the defendant’s hand samplers differ ($p < 0.0001$) from the combined characteristic GSR population from the gloves, fanny pack and truck interior. The statistical analysis is based on characteristic GSR particles with additional elements of aluminum and copper between the populations. There were no control samples taken within the facility, which had a shooting range in its cellar. The testing of the defendant’s power hammers was a waste of resources. The second prosecution expert should also have addressed the possibility of GSR contamination in the police environment.

9236-48, Session PS1

Do electron flux and solar x-ray variation in juxtaposition prior a seismic event make signature?

Umesh P. Verma, Patna Science College (India); Amitabh Sharma,

Maharani Janki Kuanr Girls Inter College (India)

Careful observations monitoring on satellite data at RT basis for electron flux and X-Ray variation directly connected with NOAA JPL Nasa and IPS AustraliaSWPC have revealed interesting information about seismic signatures. Electron flux as ionospheric proturbance is pre-distinct feature prior seismicity and shows decline in variation peak.it has been seen at the simultaneous scale X-ray (solar data) shows decline. Images taken by satellite data of these agencies on global basis at RT level provides pre-seismic information about the event of Iran 6.8 Mw on April 14,2013 and N.Zealand July16 and China August 2013 . Data states a concrete message regarding ionospheric protuberance on pre-seismic events. the facts are completely explained on Maxwell theory of Electromagnetic wave prorogation.

Electron flux variation is exposure of strain release or contraction in the electric field setup due to EM wave induced by stress accumulated at LIA contact. Although its not away from solar activity. But favorable HF system prior seismic events cancels all doubt. electric field set-up prior the event impresses the electron flux lowering by consuming available electron accumulation and thus shows lowering in data recording. at the same time strained electric field consumes electronic ions and x-Ray turned energy to provide relaxation in the system under strain. which shows X-ray decline in consuming available energy immediate prior (one or two hour) seismic events.This is conspicuous by images of these data monitored prior the events mentioned in abstract(i.e Iran 6.8mw on 14 April2013,China 28August 2013, N.Zealand ,16 July 2013 etc.)

9236-49, Session PS1

Chromium-doped ZnSe nanoparticles induced by ns laser pulse

Jiayu Yi, Guoying Feng, Chao Yang, Shouhuan Zhou, Sichuan Univ. (China)

Chromium doped ZnSe nanocrystalline particles (Cr2+:ZnSe NCPs) by using nanosecond pulsed laser ablation of polycrystalline Cr2+:ZnSe micron-sized powder in water environment are presented. The SEM and XRD results reveal that the products are ZnSe cubic sphalerite structured with an average size of 50 nm. Based on the Cr2+:ZnSe nanoparticles, typical random laser emissions centering at 2180 nm with a threshold of 0.4 mJ/pulse were observed. Compared to the Cr2+:ZnSe bulk laser, the central wavelength shows a ~ 170 nm blue-shift. With the pump energy increasing (above the threshold value), the decay time of the central wavelength reduces to 30 ns from 1.2 ?s. Meanwhile we have found that the decay time varys with the random laser wavelength. For the peak wavelength 2180 nm, the decay time is about 30 ns, while for the wavelength away from the peak position, the the decay time is 1.2 ?s. The relation between the decay time and wavelength is gradual transformation.Our experimental results demonstrate that th eCr2+:ZnSe nanoparticles random lasing emission appears in a wide pump wavelength range from 1500 to 1900 nm. We expect that this work will extend studies in areas of mid-IR random laser induced b ynanoparticles.

9236-50, Session PS1

Integrated SEM, x-ray analysis, and Raman spectroscopy for the identification of trace explosive post-blast residues

Nigel Hearns, Denis N. Laflèche, Royal Canadian Mounted Police (Canada)

Raman spectroscopy was used to characterize a variety of differnt trace explosive residues post-blast from a variety of different improvised explosive device (IED) fragments, examined in an SEM chamber and likewise characterized using EDS also. Both high- (e.g. PETN, RDX) and low- (e.g. smokeless powders, black powder) explosives were successfully characterized. Different substrates were used to simulate different construction scenarios for IED (e.g. steel vs PVC pipe). The system used was Tescan USA Vega-3 XMU Variable Pressure Scanning Electron Microscope (VP-SEM), fitted with a Renishaw SCA probe housing, an Oxford Instruments XMAX50 -XMax50 Large Area Analytical Silicon Drift Detector (SDD) with PentaFET® Precision, an Everhart-Thornley Secondary Electron Detector (SE) with YAG scintillator, a motorized retractable YAG backscattered electron detector (BSE), and a Tescan patented Low-Vacuum Secondary Electron Detector (LVSED). The Tescan used Vega Software version 3.4.2.0 and the EDX used Oxford Instrument INCA version 4.11. A 532 nm (green) excitation laser was used for all Raman experiments. Challenges and benefits will be presented.

9236-51, Session PS1

Confirmatory analysis of field-presumptive GSR test sample using SEM/EDS

Sarah Toal, Daniel D. Montgomery, Gregory S. Erikson, RedXDefense (United States); Wayne D. Niemeyer, McCrone Associates, Inc. (United States)

RedXDefense has developed an automated red-light/green-light field presumptive lead test using a sampling pad which can be subsequently processed in a Scanning Electron Microscope for GSR confirmation. The XCAT's sampling card is used to acquire a sample from a suspect's hands on the scene and give investigators an immediate presumptive as to the presence of lead from primer residue. This same sampling card can then be sent to a crime lab and processed on the SEM for GSR in the same manner as the existing tape lifts currently used in the field.

GSR field presumptive tests have historically been difficult to interpret, hazardous to the user, and consumed the field test sample. Since the amount of residue deposited on the hands from firing a weapon is shed rapidly over a short time, it may be undetectable in less than 2-4 hours after shooting. Consequently, many investigators prefer to reserve whatever amount of residue may be collected for the SEM test, which is able to confirm the presence of GSR by evaluating particle morphology and particle identity (i.e. elemental composition). However, SEM analyses are expensive and results may not be available for weeks to months, leaving a potentially useful piece of evidence unknown for some time. Therefore, the ability to use the XCAT for a field presumptive GSR test on a sample that could be further analyzed in a confirmatory test provides a useful advantage over current practices.

Sampling efficiency has been optimized by a dual sample collection approach, first by dabbing an adhesive portion of the sampling card over the hand, then by swiping a paper portion over the same area. The card is then placed into the XCAT wherein it is analyzed for lead residues via a modified rhodizonate colorimetric test. Primer residue is targeted to avoid the strongly acidic conditions typically used in propellant-detection (e.g. diphenyl amine in 70% sulfuric acid), which consume the GSR-characteristic particles and render the sample unsuitable for further SEM analysis. The non-destructive XCAT analysis allows the sample to be preserved for further confirmatory testing by sealing the card, intact as removed from the XCAT, in a plastic bag.

Detection of GSR-characteristic particles (fused lead, barium, and antimony) as small as 0.8 microns (0.5 micron resolution) has been achieved using a JEOL JSM-6480LV SEM equipped with an Oxford Instruments INCA EDS system with a 50mm2 SDD detector, 350X magnification, in low-vacuum mode and in high vacuum mode after coating with carbon in a sputter coater. GSR has been detected on samples that were exposed to the presumptive chemical test at least one-month prior, thus illustrating the stability of the particles over time. Longer term exposure studies are underway. Analysis may be done directly on the sampling adhesive, which can be easily cut from the sampling card; no specialized sample preparation is necessary.

The presumptive result provided by the XCAT yields immediate actionable intelligence to law enforcement to facilitate their investigation, without compromising the confirmatory test necessary to further support the investigation and legal case.

9236-14, Session 5

Assessing the viability of multi-column electron-beam wafer inspection for sub-20nm defects *(Invited Paper)*

Brad Thiel, SEMATECH Inc. (United States) and SUNY College of Nanoscale Science and Engineering (United States); Michael J. Lercel, Brian C. Sapp, Benjamin D. Bunday, Abraham Arceo, SEMATECH Inc. (United States)

The sensitivity of light scattering-based defect inspection technologies used in semiconductor manufacturing decreases exponentially when defects fall below ~20 nm. Accordingly, the inspection methods currently in use are beginning to experience a decline in defect capture rates. These defects include nanometer-sized extraneous particles, pattern defects from lithography, scratches, and residues. While several characterization techniques can easily meet the resolution and sensitivity requirements for such features, virtually none can do so at the throughput rates required for high volume manufacturing (HVM)—which are on the order of one wafer per hour (the current ITRS throughput target for defect inspection of wafers is 3000 cm2/hr).

Scanning electron microscopes (SEMs) can easily detect sub-20 nm features with extremely high data quality, but scanning a full 300 mm wafer at nanometer resolution would literally require months. Therefore, one solution to defect inspection would be a tool based on a massively parallel array of electron beams operating simultaneously. Two possible approaches for realizing such a technology involve assembling arrays of miniature columns and using beam splitters in conventional columns.

SEMATECH has initiated a program to assess the viability of multi-beam inspection and formulate performance specifications. In the initial phase, the critical questions are: Is the concept feasible? What are the critical system components? Does the core (column) technology exist? The first step towards determining feasibility was to develop a model for the number of beams required to achieve target throughput—dependent on operating parameters such as beam current, spot size, and pixel dwell time—for a given level of contrast between the defect and background. An important consideration in such an analysis is to remember that the objective is not to resolve the defect, but rather to detect its presence. The specific implication is that the spot size can be significantly larger than the feature, provided that the electron flux is sufficient to detect a contrast change due the defect at a given level of statistical confidence. The analysis concluded that the approach was feasible, but would require several hundred to a few thousand beams, depending on the exact spot size versus beam current performance of a given column design. Several of the core electron-optical technologies that we surveyed offered probe current-to-spot size performance that met the requirements, suggesting that the approach is feasible.

The primary questions in the second stage assessment center on the proposed system architectures: can the electron-optical column technologies be successfully arrayed? Do random and systematic variations in beam characteristics across the array fall within acceptable limits? Can a detection strategy be developed which maintains a high fidelity mapping of the signals back to their originating column or beamlet? Many of the experimental evaluations required for this stage are addressed by analyzing the contrast transfer function (CTF) for each beam, extracted from images of a specially fabricated random dot array based on 12 nm design rules. The CTF can provide quantitative information on image fidelity, information limit, detector quantum efficiency, and signal-to-noise ratio.

9236-15, Session 5

Photomask linewidth comparison by PTB and NIST

Detlef Bergmann, Bernd Bodermann, Harald Bosse, Egbert Buhr, Gaoliang Dai, Physikalisch-Technische Bundesanstalt (Germany); Ronald G. Dixson, National Institute of Standards and Technology (United States); Wolfgang Hässler-Grohne, Hai Hahm, Physikalisch-Technische Bundesanstalt (Germany); John S. Villarrubia, Andras E. Vladár, National Institute of Standards and Technology (United States); Matthias Wurm, Physikalisch-Technische Bundesanstalt (Germany)

Precise dimensional control is crucial in photomask manufacturing and the comparability of results of different measurement methods, [1] the possibility of a reference measurement method [2] and of combined or multi-tool metrology solutions, [3] i.e., using the results of different methods have been intensively discussed in recent years. Here we report on the latest results of dimensional measurements performed at PTB and NIST with different methods on a chrome-on-glass photomask.

The sample used for this bilateral comparison is a mask standard, a PTB design, [4] that was manufactured by the Advanced Mask Technology Center (AMTC) in Dresden, Germany. We have measured several features and compared their results down to the nominal 100 nm wide lines on this mask of isolated and dense, clear and opaque structures.

The linewidth or critical dimension (CD) measurements on the photomask standard were carried out by different techniques, mainly CD-AFM, by CD-SEM and transmission optical microscope characterizations. The definitions of the measurands were stated, as e.g. width of the line at 50 % of the line feature height. For every measurement method applied, a suitable model for the determination of the measurand from the microscope image has been applied. For each of the linewidth measurement results the associated measurement uncertainty values were evaluated according to accepted international guidelines [5] to allow meaningful comparisons of the results and their further use in combined (hybrid) metrology solutions. This paper presents and discusses the comparison of measurement results with their associated measurement uncertainty values.

It should be pointed out, that the bilateral photomask comparison between PTB and NIST also serves as a preparation for a future international comparison, which will include a greater number of national metrology institutes worldwide under the Mutual Recognition Arrangement of the International Committee of Weights and Measures - (CIPM-MRA) [6].

1. B. Bodermann, D. Bergmann, E. Buhr, W. Häßler-Grohne H. Bosse, J. Potzick, R. Dixson, R. Quintanilha, M. Stocker, A. Vladár, N. G. Orji: Results of an international photomask linewidth comparison of NIST and PTB; SPIE Conference on Photomask Technology 2009 Proc. of SPIE Vol. 74881H-1

2. Ndubuisi G. Orji, Ronald G. Dixson et al.: Progress on implementation of a reference measurement system based on a critical-dimension atomic force microscope, J. Micro/Nanolith. MEMS MOEMS 6(2), 023002, Apr–Jun 2007

3. N.F. Zhang, R.M. Silver, H. Zhou and B.M. Barnes. Improving optical measurement uncertainty with combined multi-tool metrology using a Bayesian approach. Applied Optics, Vol. 51, No. 25. Sept. 1, 2012

4. Richter, J., et al: “Calibration of CD mask standards for the 65 nm mode: CoG and MoSi”, EMLC 2007, 23rd European Mask and Lithography Conference EMLC, Proc. SPIE: 6533, 2007, 65330S-1 - 65330S-10

5. Guide to the expression of uncertainty in measurement, ISO, 1995, 110 p., ISBN 92-67-10188-9

6. http://www.bipm.org/en/cipm-mra/

9236-16, Session 5

Three-dimensional SEM metrology at 10nm

Andras E. Vladár, John S. Villarrubia, Bin Ming, R. Joseph Kline, Michael T. Postek, National Institute of Standards and Technology (United States)

The shape and dimensions of nanometer-scale structures are important parameters for many scientific and industrial applications. The scanning

electron microscope (SEM) is one of the instruments used in past for dimensional measurements on features 100 nm and larger. Here we are reporting results on much smaller patterns that have been measured using a model-based library SEM (MBL SEM) technique. The sample consisted of a 4-line repeating integrated circuit pattern. Lines were narrow (10 nm), asymmetric (different edge angles and significant rounding on one corner but not the other), and situated in a complex neighborhood, with neighboring lines as little as 10 nm or as much as 28 nm distant. The shape cross-section determined by this method was compared to transmission electron microscopy (TEM) and critical dimension small angle x-ray scattering (CD-SAXS) measurements of the same sample with good agreement.

A recently developed image composition method was used to obtain sharp SEM images, in which blur from vibration and drift were minimized. A Monte Carlo SEM simulator (JMONSEL) produced a model-based library that was interpolated to produce the best match to measured SEM images. Three geometrical and instrument parameterizations were tried. The first was a trapezoidal geometry. In the second one corner was significantly rounded. In the last, the electron beam was permitted to arrive with stray tilt. At each stage, the fit to the data improved by a statistically significant amount, demonstrating that the measurement remained sensitive to the new parameter. Because the measured values represent the average unit cell, the associated repeatabilities are at the tenths of a nanometer level, similar to scatterometry and other area-averaging techniques, but the SEM's native high spatial resolution also permitted observation of defects and other local departures from the average. Figure 1 below, on a 3D rendered plot, shows the fine details of the integrated circuit lines, shapes, widths, line edge and sidewall roughness, etc. are real. The lines are close to 10 nm wide with finest details at around 1 nm. In this case a single, top-down image was used for obtaining the 3D results, but the techniques used for this work can be applied to images taken from various angles, which might be necessary for more complex structures.

Table 1 Analysis of PbS at E0 = 10 keV

Parameter		Raw analytical total (mass concentration)		S
(atomic conc.)		Pb (atomic conc.)		
Mean	1.0081	0.4969	0.5031	
Relative error, %			-0.62%	0.62%
σ	0.00176	0.00083	0.00083	
σ relative	0.17%	0.17%	0.17%	
		S (mass conc.)	Pb (mass conc.)	
Single analysis		1.0047	0.1330	0.8717
Relative error			-0.74%	0.66%
k error		0.0005, 0.38%		0.0021, 0.24%
A-factor error			2.4E-5, 0.018%	0.0030, 0.35%
Z-factor error			1.9E-6, 0.0014%	0.0001, 0.012%
Combined errors			0.0005, 0.38%	0.0036, 0.42%

Table 2 Analysis of SrWO4 at E0 = 10 keV

Parameter		Raw analytical total (mass concentration)			O
(atomic conc., by stoichiometry)			Sr (atomic conc.)	W (atomic conc.)	
Mean	1.0017	0.6660	0.1678	0.1661	
Relative error, %			-0.10%	0.68%	-0.33%
σ	0.0019	0.00053	0.00065	0.00033	
σ relative	0.19%	0.80%	0.39%	0.20%	
		O (mass conc.)	Sr (mass conc.)	W (mass conc.)	
Single analysis		1.0029	0.1913	0.2627	0.5489
Relative error			0.27%	0.58%	0.16%
k error			0.0007, 0.27%	0.0009, 0.16%	
A-factor error				0.0093, 3.5%	0.0077, 1.4%
Z-factor error				2.7E-5, 0.010%	5.8E-5, 0.011%
Combined errors				0.0093, 3.5%	0.0078, 1.4%

[1] J. Goldstein et al., Scanning Electron Microscopy and X-ray Microanalysis, 3rd ed. (Springer, New York, 2003) 391.

[2] Newbury, D., SPIE Proceedings v 7729-8 (2010) 77290_F1-F9.

[3] Ritchie, N. W. M. and Newbury, D. E., and Davis, J.M., Microscopy and Microanalysis, 18 (2012) 892-904.

[4] Newbury, D. E. and Ritchie, N.W.M., SPIE Proceedings, Vol. 8036 (2011) 803601-1 - 803602-16.

[5] Ritchie, N. W. M. and Newbury, D. E., Anal. Chem., 2012, 84, 9956-9962.

9236-17, Session 6

Rigorous quantitative elemental micro-analysis by scanning electron microscopy/ energy dispersive x-ray spectrometry (SEM/ EDS)

Dale E. Newbury, Nicholas W. M. Ritchie, National Institute of Standards and Technology (United States)

Quantitative elemental microanalysis by scanning electron microscopy/ energy dispersive x-ray spectrometry (SEM/EDS) can now be performed with high accuracy for problems that involve extreme spectral overlaps [1, 2]. This performance is enabled by the silicon drift detector energy dispersive spectrometer (SDD-EDS), which can operate at high throughput (104 to 105 counts per second) while maintaining extremely stable peak shape (resolution) and position (calibration) [2]. High count spectra (106 to 107 integrated counts) that provide excellent peak statistics can be measured in modest time (100 s), and the peak stability enables accurate intensity measurements by peak fitting with the multiple linear least squares (MLLS) procedure even for severely overlapping peaks [3]. By measuring x-ray peak intensities on unknowns and standards that have been carefully polished to eliminate geometric effects on electron scattering and x-ray propagation, the rigorous standards-based method for quantitative x-ray microanalysis can be applied [1, 4]. The NIST DTSA-II EDS analysis software engine provides these calculations and supports the results with estimates of the major components of the error budget including the count statistics for unknown and standard(s) and the uncertainty estimates for the matrix (inter-element) corrections atomic number (electron scattering and retardation) and x-ray absorption [5]. Examples of the results are shown in Tables 1 (PbS, where PbM and S K are separated by 38 eV) and 2 (SrWO4, where SrL and W M are separated by 31 eV) demonstrate the accuracy that can be achieved despite severe overlaps. NIST DTSA-II is available free at: http://www.cstl.nist.gov/div837/837.02/epq/dtsa2/index.html).

9236-18, Session 6

Measurement of hypodermic needle punctures in pharmaceutical vial stoppers by light and scanning electron microscopy: a preliminary study

S. Frank Platek, Stefanie L. Kremer, U.S. Food and Drug Administration (United States)

Since its creation in 1990, the US Food and Drug Administration's Forensic Chemistry Center (FCC) has examined evidence in criminal cases related to a wide variety of product tamperings. In the mid-1990's, the FCC worked with the Indiana State Police Criminal Laboratory in a joint project to develop a method to identify hypodermic needle

punctures in rubber pharmaceutical vial stoppers related to a serial killer. The microscopy method was successful in determining the characteristic shapes of hypodermic syringe needle punctures and the minimum number of punctures in pharmaceutical vial stoppers (1).

The regularity of forensic cases related to product tampering of pharmaceuticals involving theft of controlled substances or deaths has emphasized the importance of determining the size of hypodermic needles used to commit these crimes. The ability to show the relationship between needle puncture size and the gauge of suspect hypodermic needles, which may be found at the scene or in the possession of a suspect, is often requested by investigators. These cases may include massive theft of controlled substances such as morphine and fentanyl from health care and emergency services, or deaths by injection of lethal substances into pharmaceutical vials, patient intravenous bags, and kidney dialysis administration lines.

This preliminary study investigates the use of stereoscopic and digital light microscopy as well as scanning electron microscopy to accurately measure hypodermic needle punctures in rubber stoppers of pharmaceutical vials and relate those measurements to needle gauge. The ability to determine the gauge of hypodermic needles used to create punctures combined with the identification of puncture shapes in rubber stoppers will provide additional information in the investigation of hypodermic needle-related product tampering cases.

1. S. Frank Platek, Mark A. Keisler, Nicola Ranieri, Todd W. Reynolds, and John B. Crowe. “A Method for the Determination of Syringe Needle Punctures in Rubber Stoppers Using Stereoscopic Light Microscopy” J Forensic Sci 2002;47(5):986-992.

9236-19, Session 6

First experiences with 2D-mXRF analysis of gunshot residue on garment, tissue, and cartridge cases

Alwin Knijnenberg, Amalia Stamouli, Martin Janssen, Netherlands Forensic Institute (Netherlands)

The investigation of garment and human tissue originating from a victim of a shooting incident can provide crucial information for the reconstruction of such an incident. Determining the entries and exits of bullet trajectories, the shooting distances and the elemental composition of ammunition are prime examples of such information. Current methods employed in this type of forensic investigations involve visual inspection, application of chemographic methods and other supporting techniques like SEM/EDX and FTIR. Combining the results of these methods gives valuable information on the elemental composition and distribution of gunshot residue.

Current methods however have their drawbacks. The chemographic methods have been developed for specific elements and are limited to these elements only. Moreover, the results are often greatly influenced by the presence of blood or dirt. Ideally one could use SEM/EDX to fully map the area around a bullet hole, but besides other problems such elemental mappings would be extremely time consuming. In the late 90’s the first work was published on the application of 2D-milli x-ray fluorescence (2D-mXRF) for the investigation of bullet holes and wounds [1, 2]. Together with more recent work [3-5], these results look promising in avoiding the biggest disadvantages of previously mentioned methods. 2D-mXRF has several advantages over chemographic methods and SEM/EDX as the technique can be used to scan large areas, provides simultaneous information on multiple elements starting from sodium, can be applied under ambient conditions and is non-destructive.

As 2D-mXRF is new in the forensic field, the Netherlands Forensic Institute is exploring this technique and its implementation in case investigations. In this paper we report on our experiences and challenges with the implementation of 2D-mXRF in GSR analysis. We mainly focus on the use of 2D-mXRF as a tool for visualizing elemental distributions around holes in various types of materials commonly encountered in casework.

In particular we have compared the elemental distributions acquired with 2D-mXRF with traditional chemographic methods such as sodiumrhodizonate, DTO and Zincon. Additionally we have looked into the distribution of elements found in unconventional and previously undetectable ammunitions. It is these types of ammunition where 2D-mXRF can provide important new insights since no suitable chemographic methods are available. The most important validation parameters as well as pitfalls encountered when working with 2D-mXRF on various types of matrix materials will be covered. Finally, the use of 2D-mXRF as a fast screening tool for determining the elemental composition of GSR originating from cartridge cases and a comparison with SEM/EDX will be presented.

Reference list

[1] Brazeau, J. and Wong, R.K.; Analysis of Gunshot Residues on Human Tissues and Clothing by X-Ray Microfluorescence; Journal of Forensic Sciences 1997; 42(3); 424-428.

[2] Flynn, J.; Stoilovic, M.; Lennard, C.; Prior, I. and Kobus, H.; Evaluation of X-ray microfluorescence spectrometry for the elemental analysis of firearm discharge residues; Forensic Science International 1998; 97; 21-36.

[3] Berendes, A.; Neimke, D.; Schumacher, R. and Barth, M.; A Versatile Technique for the Investigation of Gunshot Residue Patterns on Fabrics and Other Surfaces: m-XRF; Journal of Forensic Sciences 2006, 51(5), 1085-1090.

[4] Schumacher, R.; Barth, M.; Neimke, D. and Niewöhner, L.; Investigation of Gunshot Residue Patterns Using Milli-XRF Techniques: First Experiences in Casework; Proceedings of SPIE 2010; 7729; 772917.

[5] Latzel, S.; Neimke, D.; Schumacher, R.; Barth, M. and Niewöhner, L.; Shooting distance determination by m-XRF – Examples on spectra interpretation and range estimation; Forensic Science International 2012; 223; 273-278.

9236-20, Session 6

Developing a quality assurance program for gunshot primer residue analysis

Thomas R. White, Texas DPS Crime Lab. Service (United States)

No Abstract Available

9236-21, Session 6

An electro-conductive organic coating for scanning electron microscopy (déjà vu)

Bryan R. Burnett, Meixa Tech (United States)

In the late 1960s, two groups, English and German, were experimenting with electro-conductive organic coatings for use in the scanning electron microscope (1,2). The English group discovered a compound that was stable under the electron beam, can be applied with an extremely thin coating and is highly electro-conductive (1). The English company, Polaron Equipment Ltd, picked up the product and marketed it as an antistatic compound mainly for the electronics industry. The product was sold in a standard pressurized spray can (3). It appeared to have been discontinued in the early 1980s. The author obtained a can of the product in 1981, removed the product from the can when it lost pressure and stored it in a tightly sealed glass container. Over the last fifteen years he used it for viewing fabric samples in the SEM. It was thought during these years that carbon coating the samples was a necessary step for viewing in the SEM. However, recent experiments with the Polaron product indicate carbon coating is not necessary.

The product forms a polymer upon drying. Its Freon solvent is no longer available. A new solvent was developed and the product, tentatively called “ConductCoat,” will likely be available early 2015.

ConductCoat opens a new, exciting forensic application for standard SEM. It is well suited for the viewing of fabric samples and associated gunshot (GSR) residue in the SEM under high vacuum.

A fabric sample of any type is mounted on a standard GSR sampler.

Two or three drops of ConductCoat are applied to the mounted fabric sample, dabbed with a filter paper, dried for 10 minutes and placed in the SEM without additional treatment. A number of images of ConductCoat treated samples will be shown in this presentation. Individual fibers sticking out of the fabric, which often occur in such samples, are fully conductive with the ConductCoat coating regardless of the fiber length. Such fibers, if coated with only carbon or gold, charge causing image distortion or hot spots due to incomplete surface coating. Fabric pieces treated with ConductCoat are conductive throughout, whereas if coated only with gold or carbon, electrons do not have a pathway to ground and charging usually makes imaging impossible.

ConductCoat is a chlorinated hydrocarbon which adds chlorine to objects that are coated with this material.

ConductCoat eliminates the need for environmental SEMs as well as carbon or gold coating and makes it possible to quickly analyze fabric bullet rub and bore wipe GSR. Fabric samples can also be viewed for GSR from intermediate-range shots and to estimate muzzle-target distances (4).

References

1. J.Sikorski, J.A. Nott, J.S. Moss and T.Buckley. Proceedings of the Royal Microscopical Society. 1967. 2 (4): 431

2. Huber, H. Beitr. Elektronemikroskop. Direktabb. Oberfl. 1968. 1, S. 229-236.

3. Ted Pella Company, catalogue # 94, “conducting film aerosol”; ca. 1978

4. Burnett, B.R. The form of gunshot residue is modified by target impact. Journal of Forensic Sciences. 1989. 34: 808-822.

9236-22, Session 7

Using the Hitachi SEM to engage learners and promote next-generation science standards inquiry

Dave Menshew, James Enochs High School (United States)

The Hitachi TM 3000 tabletop scanning electron microscope provided an easy to use platform for high quality, meaningful student engagement. Staff were well trained by Hitachi representatives and were well qualified to deliver core concept science instruction with the device. After delivery, students were encouraged to take advantage of numerous lab hours, starting as early as 5:30 AM and included some afternoons, evenings and Saturday’s. It was found that the Hitachi TM3000 appealed across genders and ethnicities and gave a variety of students the chance to explore an otherwise unseen world.

As word spread of the device’s presence on campus, many students and teachers arrived to see it demonstrated. Those learners who first engaged became the mentors for both their peers as well as a host of interested stakeholders including the site principal, school board members, business community representatives, parents and even the County Superintendent of Schools. Throughout, students’ self-images were enhanced by virtue of having been able to master such a sophisticated (and expensive) device and then demonstrate it competently to visitors.

Images from the device were then used to give greater depth to simulated crime scene investigations that were an excellent fit with the new Next Generation Science Standards. For example, when a suspect was questioned, samples taken from his person were photographed and allowed students to form arguments about the veracity of the suspect’s travels and whereabouts. These arguments were then supported or refuted by the SEM images.

Another benefit from the use of the device in our classroom was the beginning-to-end method of investigation. Students were encouraged to develop their own hypotheses and then find samples that they could prepare, load into the device and photograph. Social media was engaged when pictures were posted online of students presenting their findings on the device. The teacher then used images in classroom teaching to further engage learners in analysis and discussions.

Before pickup, the Hitachi TM3000 was used in a cooperative investigation by our most qualified student and a pathologist with the California Dept. of Fish and Wildlife. The student drew samples from three tanks in which a total of 180 salmon were being raised for local river release. He then prepared these along with river water for viewing with the device to judge observable differences. When a mortality issue developed, the student was directed by the pathologist examine one of the eggs in the tank for parasites.

9236-23, Session 7

Integrating electron microscopy into nanoscience and materials engineering programs

Robert D. Cormia, Foothill College (United States); Michael M. Oye, NASA Ames Research Ctr. (United States)

Foothill College has developed an effective microscopy concentration within a nanoscience and materials engineering program. The program comprises training on a tabletop SEM and Atomic Force Microscope (AFM) at Foothill, and access to Field Emission (FE-SEM) and Transmission Electron Microscopy (TEM) at NASA-ASL (Advanced Studies Lab). Foothill provides basic instrument training, including basic microscopy, vacuum systems, data acquisition and image analysis. Students study materials and devices relevant in nanotechnology, and additionally use the instruments to support investigations into materials engineering. After gaining good confidence and competence level with these tools, students have an opportunity to learn basic use of the FE-SEM and TEM at NASA-ASL MACS (Materials Analysis for Collaborative Science) facility. The training at MACS is provided by a skilled operator with over two decades of microscopy experience, providing both instrument as well as advanced microscopy training.

The characterization emphasis in Foothill’s nanoscience program follows a pedagogy funded by the National Science Foundation that integrates fabrication, characterization, and design of solutions for novel applications, where students learn the integrated approach of characterization of structures, process development, and process => structure => properties optimization. The microscopy lab at Foothill is central to the materials characterization curriculum that also includes surface and elemental analysis. Students use the AFM to understand surfaces, metrology, and integration of AFM with SEM imaging. More advanced students use the FE-SEM / TEM to investigate nanostructures, including thin films, nanocarbon, and nanoparticle. Incubating innovation (I2), a novel NASA-ASL program that supports students at NASA, SJSU, and UCSC, blends materials engineering professionals with teams of students who flexibly provide and practice characterization skills to these entrepreneurial projects.

Incubating Innovation (I2) is central to two the intersection of two programs, informal education in STEM, and socialization of science, which bring together dozens of students from community colleges, undergraduate and graduate programs, and post doctoral programs. Students, staff, and faculty participate in collaborative research in the MACS facility, sharing students with skills in microscopy and fabrication, and access to instruments made available through affordable recharge rates. This program facilitates group probable solving, critical thinking, and collaboration, skills sought in the workplace. It exposes students to dozens of research projects over the course of a year, where they choose two or three to be most involved with, but still ‘collegially involved’ with the scientific and research approaches to problems in advanced materials, including biomaterials, biomedical devices, nanocarbon, using FE-SEM, TEM, and PE-CVD (Physical Organic Chemical Vapor Deposition).

The key to success of this program has been providing three tiers of instruments, Tabletop SEM, AFM, and FE-SEM and TEM, to three tiers of students, high school, community college, and undergraduate and graduate. Foothill faculty will typically train high school and community college students on the tabletop SEM, and undergraduate and graduate students on the AFM. ASL staff and research faculty train students on

the more advanced characterization and fabrications tools. The ASL environment fosters collaboration through the informally structured network of scientists, entrepreneurs, faculty researchers, and students, where the 'socialization of science' includes sharing the struggles, approaches, and insights of people with varied skills and academic maturity, and collaborative access to characterization.

Program features three tiers of microscopy:

- Tabletop SEM
- AFM
- FE-SEM/TEM

Three tiers of students:

- High school
- Community college
- Undergraduate/graduate

9236-24, Session 7

Implementation of SEM in community college and high school contexts: Hitachi's TM3000 at Ohlone College and its partner schools

Laurie Issel-Tarver, Ohlone College (United States)

Biotechnology, general biology, plant biology, and marine biology students at Ohlone College in Fremont, CA have had the opportunity in the last several semesters to examine specimens using the Hitachi TM3000 Tabletop Microscope in their labs. This microscope has allowed students to examine and measure the structures of inorganic materials, marine plankton, pollen, plant reproductive structures, leaf stomata, insects, and more. In addition, through connections with high schools that participate in Ohlone's Learning Alliance for Bioscience, high school students throughout the San Francisco Bay Area have had the chance to use the microscope. High school students in zoology, biology, chemistry, biochemistry, biotechnology, forensics, and independent research classes have taken advantage of the microscopes, both as part of their curriculum (for instance, inspecting insect samples in zoology), as well as in the interest of exploration and discovery. In addition to having the opportunity to see structures they had never seen before, through the use of the TM3000, high school and college students have learned principles of microscopy (magnification, resolution, field of view), the differences between light and electron microscopes (their sources of illumination, types of lenses), and the applications and limitations of different types of microscopes. Instructors have seen students who had been less engaged in other parts of the curriculum "come to life" when they have the opportunity to view and capture images through the TM3000.

9236-52, Session 7

Teaching the K-12 about nanoscale science by using SEM and other microscopies

Nancy Healy, Georgia Institute of Technology (United States)

The National Nanotechnology Infrastructure Network (NNIN) is an integrated partnership of 14 universities across the US funded by NSF to support nanoscale researchers. NNIN's education and outreach programs are large and varied but includes outreach to the K-12 community in the form of workshops and school programs. As part of this, we educate K-12 students and teachers about the tools of nanoscience by providing experiences with the Hitachi TM 3000 tabletop SEM. There are three of these across the network that are used in education and outreach. This presentation will discuss approaches we use to engage the K-12 community in understanding the applications of a variety of microscopes to show imaging capabilities to see both the micro and nano scales. We not only use the tabletop SEM but also include USB digital microscopes, a Keyence VHX-600 Digital Microscope, and even a small lens used with smart phones. The goal of this outreach is to educate students as well as teachers about the capabilities of the various instruments.

9236-25, Session 8

Design, technology, and application of integrated piezoresistive scanning thermal microscopy (SThM) microcantilever

Teodor P. Gotszalk, Wroclaw Univ. of Technology (Poland); Pawel Janus, Piotr B. Grabiec, Andrzej Sierakowski, Institute of Electron Technology (Poland); Guillaume Boetsch, Imina Technologies (Switzerland); Bernd Koehler, Fraunhofer IKTS-MD (Germany)

For modern nanodevices, nanostructures or nanocomposites (sub-40nm transistors, SETs, biochemical interfaces, graphene structures etc.) there is virtually no universal and multidimensional tool capable of analysing phenomena occurring in nanoscale. Wide family of AFM-based (Atomic Force Microscopy) techniques provides a various nanoscale observation techniques however the most of them are specialized and dedicated to particular types of phenomenon (mechanical, thermal, electrical). Moreover, available AFM systems do not allow for easy "domain-mixing".

In this paper, a novel micromachined, piezoresistive scanning probe microscopy (SPM) micro-cantilevers with conductive platinum tips are presented [1]. The described cantilever can be also applied in the investigations of the thermal surface properties in all Scanning Thermal Microscopy (SThM) techniques. Batch lithography/etch patterning process combined with focused ion beam (FIB) modification allows to manufacture thermally active, resistive tips with a nanometer radius of curvature (fig. 1) [2]. This design makes the proposed nanoprobes especially attractive for their application in the measurement of the thermal behavior of micro- and nanoelectronic devices [3]. Developed microcantilever is equipped with piezoresistive deflection sensor. The piezoresistive deflection detector enables metrological (in other words quantitative) analysis of interactions between the microprobe and the investigated surface. The proposed architecture of the cantilever probe enables easy its easy integration with micro- and nanomanipulators and scanning electron microscopes.

In order to approach very precisely the microcantilever near to the location to be characterized, it is mounted on a compact nanomanipulator based on a novel mobile technology. This technology allows very stable positioning, with a nanometric resolution over several centimeters which is for example useful for large samples investigations. Moreover, thanks to the vacuum-compatibility, the experiments can be carried out inside scanning electron microscopes.

The results of thermal properties studies (temperature distribution) on the surface of several micro/nanoeletronic devices using the developed integrated system will be reported.

9236-26, Session 8

Calibration transfer using a metrology atomic force microscope

Ronald G. Dixson, Natalia Farkas, John A. Dagata, National Institute of Standards and Technology (United States)

The National Institute of Standards and Technology (NIST) has a multifaceted program in atomic force microscope (AFM) dimensional metrology. A major component of this program is the development and use of intrinsically traceable instruments with displacement interferometry incorporated into the scanner. [1,2] We recently commissioned the second-generation metrology AFM at NIST: the traceable AFM (T-AFM).

One important application of these systems is to provide NIST-internal calibration support for instruments that do not have displacement traceability incorporated into the scanner. We have recently used a set of samples including both pitch and height standards for comparison and transfer purposes between our first and second generation metrology AFMs. In addition, these samples and measurements also provide traceable scale calibrations for an open-loop AFM that is used in nanoparticle metrology and research at NIST.

Our paper will describe these measurements, the associated uncertainties, and the algorithms used to accomplish the transfer.

1. J. A. Kramar, R. Dixson, N. G. Orji, "Scanning Probe Microscope Dimensional Metrology at NIST," Meas. Sci. Technol. 22, 024001, 1-11 (2011).

2. R. Dixson, D. A. Chernoff, S. Wang, T. V. Vorburger, S. L. Tan, N. G. Orji, J. Fu, "Multi-laboratory Comparison of Traceable Atomic Force Microscope Measurements of a 70 nm Grating Pitch Standard," J. Micro/Nanolith. MEMS MOEMS Vol. 10, 013015 (2011).

9236-27, Session 8

Classification of patterned wafer defects by AFM-based modulus measurement

Aaron Cordes, Martin Samayoa, SEMATECH Inc. (United States); Sean Hand, Bruker Nano Inc. (United States)

Fast, non-destructive material classification of nano-scale defects is a critical gap in many areas of semiconductor manufacturing and development, ranging from in-line high volume manufacturing to EUV mask blank development. The conventional technology used to perform this function, SEM with EDX, is fundamentally limited by signal to noise issues, leading to extreme loss of signal to noise on sub-50nm particles and defects. PeakForce Quantitative Nano-Mechanical measurement (PF-QNM) has been shown to be capable of classifying the material of particles as small as 1nm in thickness, but questions still remain regarding its ability to resolve materials of similar modulus and to operate in patterned industrial features. The present work addresses these concerned by using patterned AMAG6 test chips created in SEMATECH's Albany development facility as substrates for targeted process particle deposition using a nebulization and electrostatic filtering process. The AMAG6 chips provide both an array of realistic feature dimensions and the detailed navigation to allow specific particles to be re-acquired in the FIB for TEM analysis. Electrostatic filtering allows us to deposit multiple types of process particles into the same area, artificially filtered to remove size discrimination as a factor in material identification. The combination of these factors in turn provides a more realistic and statistically relevant test for PF-QNM's defect classification capabilities. Targeted particles sets for this work include Al2O3, Fe3O4, Fe, Cu, PSL and PMMA, in a sizes ranging from 17 to 35nm.

9236-28, Session 8

Deformation effects in accurate nanoparticle metrology with atomic force microscopy

Malcolm A. Lawn, Jan Herrmann, Victoria A. Coleman, Bakir Babice, Åsa K. Jamting, National Measurement Institute of Australia (Australia)

Nanoparticle metrology with atomic force microscopy (AFM) is based on a relatively simple, idealised measurement model in which the diameter of a particle is often derived from the measured difference in height between the apex of the particle and the mean level of a flat substrate to which the particle is attached. Measuring the particle diameter vertically avoids inaccuracies introduced by tip broadening of the particle image in the lateral plane.

One assumption of this model is that the particles are not deformable; however recent studies have demonstrated that in the case of commonly used polystyrene latex reference nanoparticles, particle deformation results in a significant measurement offset and uncertainty. Particle deformation may contribute to the method divergence observed in laboratory comparisons between AFM and other commonly used nanoparticle sizing techniques such as transmission electron microscopy, dynamic light scattering and differential centrifugal sedimentation, where the AFM particle diameter measurements are smaller than those from these other techniques.

The aim of this study is to investigate how dimensional measurements of commonly used reference nanoparticles are influenced by the force exerted by the AFM tip during the image acquisition process. A better understanding of these measurements is important not only for the accurate measurement of nanoparticle reference materials but also for the accurate characterisation of more complex nanomaterial systems.

The force exerted by an AFM tip on the surface being measured depends on the imaging mode and the set point of the feedback loop. Intermittent contact (or "tapping") mode AFM is most commonly recommended for nanoparticle imaging and metrology. In this mode, the downward force exerted by the tip on the sample is controlled by the set point of the instrument's feedback loop. The set point is expressed as a percentage of the AFM cantilever's free air amplitude i.e. the lower the set point, the greater the force exerted by the tip.

We report on a series of experiments in which the mean diameters of some commonly used commercially available nanoparticle reference materials are imaged and measured with a range of free-air amplitude and set point combinations, in intermittent contact mode. The results demonstrate that tip force during imaging does cause measurable plastic deformation of nanoparticles. The amount of deformation varies with particle size, with the mean measured diameter of nominally 5.5 nm diameter gold reference material nanoparticles being reduced by as much as 50%. Plastic deformation of particles is demonstrated by the comparison of measurements derived from repeated imaging of the same sample area with measurements (using the same imaging parameters) derived from sample areas not previously imaged.

9236-29, Session 8

Use of a tip characterizer in atomic-force microscopy nanoparticle size analysis: correlated height and width measurements

Natalia Farkas, Ndubuisi George Orji, Ronald G. Dixson, National Institute of Standards and Technology (United States); Hiroshi Itoh, National Institute of Advanced Industrial Science and Technology (Japan); John A. Dagata, National Institute of Standards and Technology (United States)

Polystyrene latex (PSL) spheres are one of the most important nanoparticle reference materials available. Recently however, Garnaes [1] pointed out the complicated nature of uncertainty estimation for atomic force microscopy (AFM) measurements of polystyrene latex (PSL) reference spheres.

In the traditional approach to AFM particle metrology, a single dimensional measurand is considered to be prudent, either a mean value of the particle diameter based on the particle height or an average width obtained from a line average of a 2-dimensional particle lattice. We propose that a measurement model based on correlated height and width measurements of individual, discrete particles resolves contributions from particle-substrate deformation, which occurs during sample preparation, and particle-probe deformation, which occurs during imaging [2].

Our proposed model necessarily involves additional effort to characterize the AFM probe tip. To do so, we have employed a novel tip characterizer based on an Si/SiO2 multilayer structure that has been validated for standard AFM probe shapes [3-4] as well as for critical-dimension (CD) type probes [5]. This talk summarizes our experience using the characterizer to establish limits for the variation of AFM probe shape for analysis of individual particle cross-sections and statistical correlation of many-particle data.

1. J. Garnaes, Meas. Sci. Technol. 22 094001 (2011).

2. J. A. Dagata et al., manuscript in preparation.

3. H. Itoh, T. Fujimoto, and S. Ichimura, Rev. Sci. Instrum. 77 103704-1 (2006).

4. H. Takenaka et al., e-J. Surf. Sci. Nanotech, 9 293 (2011).

5. N. G. Orji and H. Itoh, manuscript in preparation.

9236-30, Session 8

Particle deformation induced by AFM tapping under different set-point voltages

Chung-Lin Wu, Industrial Technology Research Institute (Taiwan); Natalia Farkas, John A. Dagata, National Institute of Standards and Technology (United States); Bo-Ching He, Wei-En Fu, Industrial Technology Research Institute (Taiwan)

Atomic force microscopy (AFM) is one of the tools frequently used for measuring the diameter of nanoparticles. The intended measurand (defined inVIM3 [1]), the particle diameter, is typically taken to be the maximum height of the particle relative to the substrate upon which it is attached. Height measured in this way coincides with the actual particle diameter only if the particle is incompressible. However, it is now accepted that deformation induced by AFM contact or tapping forces can occur in the case of some important nanoparticle reference materials [2]. In this presentation, this influence quantity is studied by controlling the operational AFM setpoint voltage (SPV) during AFM tapping-mode imaging of polystyrene nanoparticles.

Well dispersed nominal 60-nm NIST polystyrene latex (PSL) standard reference materials (SRM 1964) and 60-nm BBI gold nanoparticles were co-adsorbed on poly-L-lysine coated mica substrates. Topography and phase images of isolated nanoparticles were scanned at an initial SPV optimized for high-quality AFM tapping-mode imaging. In order to observe PSL deformation characteristics, the initial SPV was reduced in a step-wise fashion and an image containing both PSL and gold particles was obtained at that SPV. Figure 1(a) shows the topographic height image of mixed nanoparticles using the initial SPV. It is difficult to distinguish PSL and gold nanoparticles in this image, since both nanoparticles are of similar shape and dimension. On the other hand, the two particle types are readily identified in an AFM phase image on the basis of faceting of the gold nanoparticles, as shown in Figure 1(b).

An image stack collected as a function of SPV is analyzed using cross-sectional data for a large number of individual PSL and gold particles, presented in Figure 2 as height vs. SPV. As the SPV is reduced, the height of compressible PSL nanoparticles is seen to decrease. In contrast, the height of co-adsorbed gold nanoparticles adjacent to the PSLs is unaffected by the value of SPVs used for imaging. This result demonstrates that gold nanoparticles are incompressible (to within +/- 0.2 nm) and a significant deformation of several nanometers, especially for smaller sized particles, may occur in the case of PSLs. In the course of this work, we have identified the range of SPV values over which no deformation occurs, i.e., within a narrow window around the optimal imaging setpoint, as well as the yield point, i.e., the cross-over from elastic to plastic deformation at reduced setpoint value.

In summary, the effect of setpoint voltage on height measurements of PSL SRMs during AFM tapping-mode imaging was observed using co-adsorbed SPL and gold nanoparticles. It was found that the deformation of polystyrene nanoparticles increased with decreasing setpoint, whereas there was essentially no deformation of gold nanoparticles. Rigorous monitoring and control of the SPV so that it remains within a narrow operating range for optimal AFM tapping-mode imaging is essential for establishing a minimal and meaningful uncertainty estimate in AFM metrology of PSL reference materials.

References

[1] BIPM/JCGM (2008), International Vocabulary of Metrology, 3rd ed.

[2] J. Garnaes, Meas. Sci. Technol 22 094001 (2011).

9236-31, Session 9

Wavelet transform-based method of compensating dispersion for high-resolution imaging in SDOCT

Haiyi Bian, Wanrong Gao, Nanjing Univ. of Science and Technology (China)

The axial resolution is an important parameter in Optical Coherence Tomography. Optical Coherence Tomography uses broadband light source to achieve axial image resolution on the few micron scale. But it is well known that the dispersion causes a broadening of the coherence envelope, therefore the dispersion mismatch between reference and sample arm needs to be minimized to achieve optimal axial resolution for OCT using broadband light source. To obtain high quality images, a number of dispersion compensation methods have been proposed. We propose a new numerical dispersion compensation method to obtain ultrahigh resolution in SDOCT. By use of wavelet transform instead of Fourier transform, we can obtain the signal in different frequency domain. And a series of the phase signals of different interface of the sample can be obtained. As we all know, if the sample is a homogeneous medium, the phase signal is a linear function of the wavelength. So by linearization of the phase signal of different interface and the wavelength, the axial resolution can be improved. The cover glass is used to verify the numerical dispersion compensation method. And the result of the experiment is satisfactory.

9236-32, Session 9

Optical coherence microscopy with extended depth of focus

Xinyu Liu, Dongyao Cui, Xiaojun Yu, Jun Gu, Ding Sun, Linbo Liu, Nanyang Technological Univ. (Singapore)

Optical Coherence Microscopy (OCM) is a combination of low coherence interferometry (LCI) and Confocal Reflectance Microscopy (CRM). The axial and transverse resolution of an OCM system is normally decoupled: the axial resolution is defined by the coherence length of the light source and the transverse resolution is defined by the Confocal focusing optics. To achieve higher axial resolution, one can always use a light source with larger spectral bandwidth without significantly affecting other performances. However, to improve transverse resolution is complicated since there is an inherent trade-off between transverse resolution and the depth of focus (DOF). Being a three-dimensional imaging tool, large DOF is highly desired, therefore, there is a call for novel techniques that can improve transverse resolution without compromising DOF.

In order to achieve high spatial resolution along large DOF, there have been a few methods proposed, such as apodizing amplitude and phase pupil filters and axicon lens. However, all these methods are associated with inherent issues with sensitivity and side lobes. For example, axicon based OCM system is 20dB less sensitive than a standard OCM system, which precludes its applications for high speed or in vivo purposes. In addition, as OCM images are normally displayed in log scale, even small side lobes will show up as pronounced image artifacts.

We have developed a new OCM system based on chromatic focal shift of the collimation lens and objective lens. We have characterized the spatial resolution and DOF of the proposed OCM using a resolution chart. The sensitivity of the system is also calculated and measured. It has been demonstrated theoretically and experimentally that an 8-fold gain in DOF can be achieved without significantly compromising spatial resolution, focus quality, and system sensitivity. The merits of the new OCM system were tested in biological tissue samples in comparison with a standard OCM. In conclusion, the proposed OCM technology is capable of achieving high spatial resolution along a much extended DOF, which is free of side lobes and does not significantly compromise sensitivity of the imaging setup.

9236-33, Session 9

Nanoscale investigations by fluorescence and scattering scanning near-field optical microscopy

Stefan G. Stanciu, Univ. Politehnica of Bucharest (Romania); Loredana Latterini, Univ. degli Studi di Perugia (Italy); Radu Hristu, Denis E. Tranca, Univ. Politehnica of Bucharest (Romania);

Luigi Tarpani, Univ. degli Studi di Perugia (Italy); George A. Stanciu, Univ. Politehnica of Bucharest (Romania)

It is well known that the spatial resolution attainable with conventional optical microscopy techniques is limited to approximately half the wavelength of the light used for excitation. For visible radiation this translates to a theoretical resolution limit of ~200 nm. These limitations motivated the development of higher resolution techniques. The first idea on how to circumvent the resolution limitations of light microscopy connected to diffraction belonged to Synge [1]. The scanning near-field optical microscope (SNOM or NSOM) is a concept that combines scanning probe techniques and optical microscopy, and in this moment is regarded as one of the key instruments in near field optics. In near field optics the bandwidth of the spatial frequencies is no longer limited by the Abbe criteria. In these circumstances, the resolution dependance on the wavelength is replaced by a dependence on the aperture diameter or tip shape and size. The highest resolution achieved by using near field microscopy, was obtained by using an apertureless scanning near field optical microscope (a-SNOM). The first SNOM systems using this principle used metalized AFM probes to create an optical „nano-focus". The size of this nano-focus depends only on the tip apex radius, providing a resolution in the order of 10 nm [2-3]. The imaging mechanism in a-SNOM is based on the optical interaction between the tip and the sample, mediated by the evanescent fields. This interaction modifies the amplitude/phase of the light waves scattered by the tip and detected by far field methods.

In this presentation we describe recent fluorescence and plasmonic scattering investigations that our group has conducted by using a commercial AFM that was in-house upgraded to perform apertureless SNOM imaging. The investigations extend previous results of our group on a-SNOM imaging of metallic and biological samples [4,5].

The presented results refer to investigations on biomaterials' surface charge and on Au-coated semiconductor nanocrystals [6,7]. A correlation between micro and nanoscale images was targeted, and fluorescence data is discussed in connection with plasmonic scattering data. The information collected by a-SNOM is correlated with AFM topography and with confocal scanning laser microscopy data.

[1] E. H. Synge, A suggested model for extending microscopic resolution into the ultra-microscopic region, Phil. Mag., vol. 6, pp. 356–362, (1928)

[2] F. Zenhausern, M. Oboyle and H. Wickramasinghe, Apertureless near-filed optical microscope, Appl. Phys. Lett. 65(13), 1623-1625 (1994).

[3] Y. Inouye and S. Kawata, Near-field scanning opticla microscope with a metallic probe tip, Opt. Lett 19(3), 159-161 (1994).

[4] G. A. Stanciu, C. Stoichita, R. Hristu, S. G. Stanciu, D. E. Tranca and T. A.M. Syed , Metalic samples investigated by using a s-SNOM near field optical microscope, Proceedings of the 14th International Conference on Transparent Optical Networks (ICTON 2012), 2-5 July 2012 , Warwick, UK;

[5] G. A. Stanciu, D.E. Tranca, R. Hristu, C. Stoichita and S.G. Stanciu , Investigations at nanoscale by using fluorescence in apertureless scanning near field microscopy, Proceedings, ICTON 2013, Cartagena, Spain, June 23-27, 2013.

[6] L. Tarpani, L. Latterini, Effect of metal nanoparticles on the photophysical behaviour of dye-silica conjugates., Photochem. Photobiol. Sci., 2014, DOI: 10.1039/C3PP50450F;

[7] L. Latterini, L. Tarpani, Hierarchical Assembly of Nanostructures to Decouple Fluorescence and Photothermal Effect J. Phys. Chem. C, 2011, 115, 21098-21104.

9236-34, Session 9

Scan mirrors relay for high-resolution laser scanning systems

David Kessler, Kessler Optics & Photonics Solutions, Ltd. (United States)

Two dimensional beam deflection is often required in medical laser scanning systems such as OCT or confocal microscopy. Commonly two linear galvo mirrors are used for performance in terms of their large apertures and scan angles. The galvo mirrors are placed at the vicinity of entrance pupil of the scan lens with a "displacement distance" separating them. This distance limits the scan fields and/or reduces the effective aperture of the scan lens. Another option is to use a beam or pupil relay, and image one galvo mirror onto the other. However, beam (or pupil) relays are notoriously complicated, expensive and can add significant aberrations.

This paper discusses a simple, all reflective, diffraction limited, color corrected, beam relay, capable of large scan angles and large deflecting mirrors.

The design is based on a unique combination of an Offner configuration with a Schmidt aspheric corrector. The design is highly corrected up to large scan mirrors and large scan angles down to milliwaves of aberrations. It allows significantly larger scan field and or scan lenses with higher numerical aperture as compared with scanners using galvos separated by the displacement distance. While this relay is of exceptionally high performance, it has one element located where the beam is focused which may present a problem for high power lasers. Thus a modification of the above design is introduced where the beam is focused in mid air thus making it usable for high power systems such including laser marking and fabrication systems. Also shown are systems using MEMs mirrors instead of galvo mirrors.

9236-35, Session 10

Using scanning near-field microscopy to study photo-induced mass motions in azobenzene containing thin films

Anh-Duc Vu, Nicolas Desboeufs, Ecole Polytechnique (France); Filippo Fabbri, Univ. Paris-Sud 11 (France); Jean-Pierre Boilot, Thierry Gacoin, Khalid Lahlil, Yves Lassailly, Lucio Martinelli, Jacques Peretti, Ecole Polytechnique (France)

Photochromic materials containing azobenzene derivatives exhibit spectacular photomechanical properties which allow the formation of surface relieves upon illumination in the chromophore visible absorption band.1,2 The size and shape of the photo-induced surface pattern can be easily adjusted over a large scale ranging from a few tens of nanometers up to several microns by controlling the projected optical pattern.3,4 The control of the photo-induced mass motion in azobenzene containing materials can be exploited for various applications, including photo-mechanical actuation, diffraction optics, holographic recording, and surface micro- or nano-patterning.

In this context, scanning near-field microscopy (SNOM) is a particularly adapted tool since it allows to detect simultaneously, in real-time, in-situ and at nanoscale, both the optical image and the surface topography. Moreover, the optical fiber probe can be used to apply a mechanical force, to disturb the local optical field or eventually as a nanoscale light source, giving another possibility of tuning the photo-mechanical process taking place in azobenzene containing films.

We will present two examples which illustrate the use of SNOM for studying the photoinduced surface deformation of azobenzene containing films. In the first example, the film is used as photoactive substrate for non-contact and non-destructive optical patterning process. SNOM allows to establish a correlation between the light pattern and the resulting deformation. It can also obtain in-situ information on the shape and size of the surface structure which is necessary to determine the sufficient dose of illumination in each surface patterning step. Using this technique, metal/dielectric hybrid 1D or 2D structures were elaborated whose optical and mechanical properties can be controlled by light. In the second example, SNOM, together with optical illumination, are used to modify the local surface structure at nanoscale. We will discuss the separate role of the optical probe and the illumination in this process.

1. P. Rochon, E. Batalla, and A. Natansohn, Appl. Phys. Lett. 66, 136 (1995).

2. K. Yang, S. Yang, J. Kumar, Phys. Rev. B 73, 1 (2006).

3. N. Landraud, et al., Appl. Phys. Lett. 79, 4562 (2001).

4. F. Fabbri, et al., J. Phys. Chem. B 115, 1363 (2011).

9236-36, Session 10

Effect of the temporal fluctuations of phase on the characterization of LCOS

Spozmai Panezai, Dayong Wang, Jie Zhao, Yunxin Wang, Lu Rong, Beijing Univ. of Technology (China)

The advancements in the development of spatial light modulators (SLMs) technology, have contributed enormously to various applications in photonics such as optical image processing, holographic data storage, programmable adaptive optics, diffractive optics and optical metrology etc. Among different spatial light modulators technologies the parallel align nematic liquid crystal spatial light modulator LCoS (PA-LCOS) enjoys special attention due to its high spatial resolution, high diffraction efficiency and phase only modulation without having coupled amplitude modulation. They act as a variable linear retarders when illuminated by linearly polarized light along the orientation of the LC director axis, no depolarization effect is available; however, they may still exhibit phase fluctuations.

These fluctuations are produced in time intervals smaller than the LCOS frame period, due to the way the electrical signal is addressed to the LCOS display and results in a temporal fluctuation of the voltage signal applied to each pixel. The use of LCDs to display phase-only diffractive elements is based on achieving a phase-only modulation configuration, where the display modifies the phase of the incoming light beam controlled through the addressed gray level, therefore for their optimal use, a proper calibration of their modulation capabilities is required.

In this paper we provide evidence of the temporal fluctuations of the phase modulation property of a liquid crystal on silicon (LCOS) display by using the conventional interferometric techniques. The various kinds of interferometric methods such as Michelson, Double slit and Mach–Zehnder are used for the characterization of LCOS by displaying different gray levels (0-255) on the LCOS with the step change of 10 gray level and their results are compared with each other. We have also analyzed how these results differ from each other due to the fluctuation of phase and other mechanical effects. Thereafter, effects are also studied for the single gray level. For this purpose a number of images are recorded for single gray level displayed on LCOS with fast CCD camera and their affect on the modulation of phase value are calculated with the variation of time. In the present study, the interferometric technique is used to quantitatively analyze the phase fluctuation with variation of time. These all comparisons and measurements are found very helpful in finding out the accurate value of total phase modulation offered by LCOS and also useful in increasing the efficiency of LCOS as DOE in optical experiments.

9236-37, Session 10

Nanoscale imaging by micro-cavity scanning microscopy

Andrea Di Donato, G. Ippoliti, Tullio Rozzi, Davide Mencarelli, G. Orlando, Marco Farina, Univ. Politecnica delle Marche (Italy)

Thanks to their high sensitivity, optical cavities have always been exploited to measure refractive index of optical glasses, to realize sensors with sub-nanometer resolution, and lastly in scanning probe microscopy to monitor the displacement of cantilevers. This work describes a scanning probe microscopy technique based on optical fiber micro-cavity, in which a cleaved single mode fiber is approached to a surface under investigation. The interaction between the sample and probe occurs at distance of tens of microns. The interfering signal directly comes from the micro-cavity in which the diffracted field experiences multiple reflections and interferences. Contrast phase images, reflectivity and topographic information can be investigated by means of the optical fiber itself without the use of lens. Variations of cavity response are induced by changes of the surface permittivity and micro-cavity dimension. Although the technique proposed features some analogies with similar scanning techniques, such as Synthetic Aperture Radars, Spectral Optical Coherence Tomography (OCT) or Scanning Near-Field Optical Microscopy (SNOM), it has some aspects that distinguish it from these. In this scanning system, no reference beam is present and the signal directly comes from the micro-cavity in which the interference phenomenon takes place due to the multiple reflections and interferences of the diffracted field from fiber facet. Only in the limit of very low reflective surfaces, the interfering signal can be described by the same analytical model on which are based OCT systems. The optical cavity was described by introducing an electromagnetic model with the aim to disentangle the sample topography from surface refractive index. The transverse resolution is not defined by the NA of fiber and consequently by the conventional Rayleigh limit, but it is a function of the transverse electromagnetic field inside the micro-cavity. Along the normal direction the resolution is affected mainly by laser source bandwidth and fluctuations or by piezo-scanner drift that affects the scans in the constant height. The spectrum acquired can be analyzed either in time domain or in frequency domain. In the latter a de-convolution model is applied according to the electromagnetic model defined in order to disentangle the topography and surface refractive index. The lens-free system paves the way towards quantitative measurements in air and liquid environment. Compared with other scanning probe microscopy techniques, the system is totally non-invasive, as it works at long range of interaction, and it does not require a special preparation of the samples. This approach is also attracting since it allows to conjugate non-invasivity and sub-diffraction imaging in liquid environment.

9236-38, Session 10

Generating the longitudinal electric-field component on the optical axis with high-numerical-aperture binary axicons

Sergei V. Alferov, Samara State Aerospace Univ. (Russian Federation); Svetlana N. Khonina, Sergei V. Karpeev, Image Processing Systems Institute (Russian Federation); Dmitrey Andreevich Savelyev, IPSI (Russian Federation)

We conduct an analytical and numerical study of the diffraction of linearly and circularly polarized laser beams by three types of binary diffractive axicons (axisymmetric, spiral and bi-axicon) with the objective to single out the longitudinal electric field (E-field) component [1-3] on the optical axis. The numerical simulation was based on the Mansuripur's modification of the PWE method [4] with regard for the Fresnel transmission coefficients and the finite-difference time-domain (FDTM) method implemented using a free-software package Meep. The experiments were conducted with high numerical aperture (NA=0.8) binary axicons fabricated by electron lithography. The near-field diffraction pattern was recorded using a near-field microscope NT-MDT equipped with a metalized fiber probe with an aperture, enabling the measurement of both longitudinal and transverse E-field components [5]. However considering that the technique is three times as sensitive to the longitudinal component when compared with the transverse one [6], the longitudinal E-field component can be reliably recorded.

We have shown that for a linearly polarized beam incident on the bi-axicon, the proportion of energy on the optical axis accounted for by the longitudinal E-field component can be controlled by rotating the optical element. For a circularly polarized beam, the bi-axicon allows one to form on the optical axis the longitudinal component independent of the optical element orientation or the polarization direction. For the spiral axicon, on the contrary, the diffraction pattern has been shown to depend on the circular polarization direction – for the opposite directions of polarization and spiral the central focal spot is predominantly formed by the longitudinal E-field component, whereas the coincident direction of polarization and spiral results in the zero central intensity. With a linearly polarized beam, the spiral axicon ensures the presence of the longitudinal component in the center of the diffraction pattern irrespective of the mutual orientation of the optical element and the polarization axis.

9236-39, Session 11

Three-dimensional Monte Carlo modeling of critical dimension SEM metrology in a TCAD simulation environment

Mauro Ciappa, Emre Ilgünsatiroglu, Alexey Y. Illarionov, ETH Zürich (Switzerland)

Nowadays, the main problems to be solved by Monte Carlo (MC) modeling of Critical Dimension Scanning Electron Microscopy (CD-SEM) are the assessment of the physical limits of the technique for nanostructures, the extraction of CD from arbitrary photoresist structures, the estimation of the line edge roughness (LER) parameters, quantification of the impact of proximity effects, dosimetry to control photoresist shrinking and temperature, accounting for self-charging effects, and energy spectral capabilities. All these challenges require an increased accuracy in the description of the three-dimensional model geometry, as well as consistent definition of the local electro-magnetic fields at nanometer scale. Traditionally, the major practical limit of such a simulation approach is the long calculation time due to particle tracking. In addition, modeling complex geometries and accounting for self-charging effects imposes the use of multiple tools to edit the geometry by hand, to mesh the structure, and to solve the Poisson equation (usually under severe limitations). Therefore, MC simulations are often carried out on uncharged samples, only, that are modeled by sparse basic body geometries, in spite of the fact that real samples are complex and dense 3D volumes with heavily textured surfaces.

In present paper, it is shown how complex photoresist sample models can be described by up to 1,5 millions unstructured tetrahedra, which are generated either in a CAD editor by meshing, or directly imported from a commercial TCAD lithography simulator. Electric fields are calculated by solving the 3D Poisson equation in a commercial TCAD environment under arbitrary boundary conditions and materials. Once computed, this information is transferred to the Monte Carlo Integrated Electron Beam Simulator (IES) developed at the ETH Zurich, which uses a multiple collision scheme for interactions at very low energies, optimized electron tracking algorithms, and high-performance computing strategies to achieve simulation times that are fully compatible with an industrial application.

In Section 1 of the paper, a benchmark structure is simulated to quantify the calculation time observed under different conditions. In particular, it is shown that, thanks to the use dedicated hierarchical structures, of the simulation time of densely meshed sample models is just a factor of two larger than the simulation time of sample models described by basic bodies. In Section 2, realistic photoresist structures (LER) in the nanometer range generated by a TCAD lithography simulator (up to 1,000,000 tetrahedra) are investigated. The critical dimensions and the roughness of the simulated structures are extracted according to a shape-sensitive library-based procedure and compared with the values obtained by the level threshold criterion. Finally, in Section 3, IES will is used in conjunction with a device simulator, to simulate self-charging and track electrons in the electrostatic field. In addition, the same procedure is applied to calculate the secondary electron energy distribution (energy spectroscopy) arising from biased and unbiased doped semiconductor structures.

9236-40, Session 11

Monte Carlo modeling in a TCAD environment for the simulation of scanning electron microscopy images of three-dimensional samples with space charge

Mauro Ciappa, Alexey Y. Illarionov, Emre Ilgünsatiroglu, ETH Zürich (Switzerland)

The build up of space charge in the samples and of the related electric fields strongly affects the formation of images in scanning electron microscopy. Therefore, Monte Carlo (MC) simulations of SEM images have to account for the physical processes that lead to the formation of a space charge, as well as for the tracking of primary and secondary electrons in the related electrostatic field.

In present work, space charges are considered, which are generated either by self-charging of dielectric samples during irradiation, or by the built-in potential in semiconductor materials.

Simulations are carried out by the Integrated Electron Beam Simulator (IES) developed at the ETH Zurich. The simulation procedure consists of four steps. In a first phase, three-dimensional samples (geometry, materials, doping, boundary conditions) are defined in a TCAD environment and the 3D geometry model is properly meshed (unstructured tetrahedron mesh). As an alternative, simulation models can be also imported from process or lithography TCAD simulation tools.

The subsequent step accounts for the calculation of space charge build up process. In the case of self-charging of dielectric materials, a quasi-static approach is considered, i.e. it is assumed that the irradiated sample has reached a steady-state charge distribution, which is not influenced by further irradiation. For this scope, the MC simulation is first used to calculate the 3D (positive and negative) charge distributions arising from the interaction of the electron beam with the dielectrics in the sample. In the case of semiconductor samples, the space charge is calculated by solving numerically the semiconductor equations in a TCAD device simulation environment. Dielectric and semiconductor materials can be present in the same sample. In the third step, the Poisson equation is solved numerically in a TCAD device simulation tool accounting for the 3D space charge, as well as for the boundary conditions of the SEM chamber (including e.g. the extraction field). Additional effects like polarization of the dielectrics are also considered. The electric field, which has been calculated in the vacuum, as well as in the different materials, is then passed to the MC simulator. Finally, a full MC simulation is carried out, which includes tracking of primary and secondary electrons in the electric field. Trajectories are calculated based on the Lorentz force for an electron motion in arbitrary static electric field in the vacuum and in the sample materials. The implemented detectors also provide energy spectroscopy capability.

The first section of this work deals with the dynamics and numerics of the dedicated algorithms implemented for electron tracking in electric field. Special attention is paid to their numerical stability. In the second section, examples are presented that focus on the simulation of SEM images of samples with space charges generated either by self-charging, or by dopant distributions in silicon. Particular focus is set to the investigation of SEM images of homo- and heterojunctions , with and without energy filtering of the secondary electrons.

9236-41, Session 11

Monte Carlo simulation of phantom tissue under dynamic spatial frequency domain imaging (DSFDI)

Jose E. Calderon, David Serrano, Jayanta Baneerjee, Univ. de Puerto Rico Mayagüez (United States)

Using Monte Carlo simulation to solve for the non-steady state in Spatial Frequency Domain Imaging. Special case diffuse optical spectroscopy imaging for wide-field optical property mapping applies pattern illumination in the spatial domain. We introduce a modified dynamic hyperbolic pattern allowing to introduce a temporal parameter in the theoretical diffusion equation. Absorption and reduce scattering was rendered using a Monte-Carlo tissue phantom model. Parallel algorithm use CUDA language code and computational engine by Graphic processing Unit (GPU) and Computer Processing Unit (CPU). Using computer simulation software show rapid process controller computer vision to assist the manipulation of devise mechanisms.

9236-42, Session 11

A compact physical CD-SEM simulator for IC photolithography modeling applications

Chao Fang, Mark D. Smith, John J. Biafore, Alessandro VaglioPret, Stewart A. Robertson, KLA-Tencor Texas (United States)

Scanning Electron Microscopy (SEM) has been widely used to measure Critical Dimensions (CD) in semiconductor lithography processes. As the size of transistors keeps shrinking, the uncertainty associated with CD-SEM accounts for a fast growing contributor to the entire metrology error budget. 3-D transistor such as FinFET also requires better profile control, which adds even greater challenges for metrology. Capability to predict the metrology results from a CD-SEM is highly desirable to reduce the uncertainty of metrology.

Simulation has been proved to be a valuable means of studying SEM metrology. Monte-Carlo based simulators are generally used to model the detailed image formation process of a CD-SEM. However, the high computational cost limits the application of Monte-Carlo based CD-SEM simulations. Typical 2D CD-SEM image simulation by a Monte-Carlo based simulator often takes at an hour or more, even on a cluster. By contrast, most rigorous photolithography process simulations take only minutes or seconds. This speed gap between lithography simulation and CD-SEM imaging simulation prevents the integration of Monte-Carlo based SEM simulators into commercial lithography simulation packages. On the other hand, simple geometric SEM models usually over-simplify the physical process of SEM imaging and lose the predictive capability in some cases. It is highly desirable to have a simulator which includes a physical model of SEM imaging, but also runs at a similar speed as a main stream lithography simulator.

We present here a compact physical CD-SEM simulator which simplifies the image formation process while preserving many essential SEM imaging mechanisms. For example, our simulator takes into account the material contrast, geometric contrast, beam spot size, beam landing energy, and electron shot noise. The shadowing effects due to surface topography are also simulated. The metrology algorithms of CD-SEM are also included in the simulator. For example, the threshold edge detection method is included as well as a few filters for noise reduction, such as Gaussian smoothing along the direction on a line scan and summing lines for averaging perpendicular to the scan direction. This CD-SEM simulator is integrated in PROLITH (KLA-Tencor, Milpitas, CA), which is a rigorous, physics-based lithography simulator, to generate the synthetic CD-SEM image. For simplification and computational efficiency, not all the physics of SEM are included, such as electron optics and detectors, charging, resist shrinkage, etc. The results of our simulator are compared with Monte-Carlo based SEM simulations by extracting and comparing line scans from both simulators as a validation. Several applications of our CD-SEM simulator are presented to demonstrate the predicting capability against experiments. First, we will present a simulated CD-SEM image of an elbow shaped OPC structure. Second, we will show the effect of side wall angle on lithography results using CD-SEM simulation and metrology. The third example will be a study of CD measurements of lithography features printed on wafers with underlying topography. Finally, we will discuss the future work needed to improve this compact CD-SEM simulator.